statistically indistinguishable from data produced by Method 29 for multielements and the Ontario Hydro Mercury Speciation Method for mercury species.

3.4 CO_2 Removal

Existing energy utilization systems are largely based on the combustion of fossil fuels in stationary and mobile devices. The increased CO_2 concentration in the atmosphere due to emissions of CO_2 from fossil fuel combustion has caused concerns for global warming (Reuther, 1999). Improving the efficiency of energy utilization and increasing the use of low-carbon energy sources are considered to be potential ways to reduce CO_2 emissions (DOE, 1999a). CO_2 capture and sequestration have been receiving significant attention and are being recognized as a third option (DOE, 1998b). Also, enriched CO_2 streams can be an important starting material for synthetic clean fuels and chemicals (Song, 2002). For carbon sequestration, the costs for capture and separation are estimated to comprise about three-fourths of the total costs of ocean or geologic sequestration (DOE, 1998b). It is therefore important to explore new approaches for CO_2 separation.

There are chemical and physical methods for separation of CO_2 from gas mixtures. Adsorption is one of the promising methods that could be applicable for separating CO_2 from gas mixtures. Various adsorbents, such as zeolites, activated carbons, carbon molecular sieves, pillared clays, and metal oxides have been investigated. At lower temperatures (e.g., room temperature), the zeolite-based adsorbents and activated carbon have generally been found to show higher adsorption capacity. However, their selectivity to CO_2 in the presence of other gases (N_2, etc.) is still low and their adsorption capacities rapidly decline with increasing temperature above 30°C, becoming negligible at temperature in excess of 200°C. It has been reported that the CO_2 adsorption capacity for zeolite 13X, 4A and activated carbon is approximately 160, 135 and 110 mg/g-adsorbent, respectively, at 25°C and 1 atm CO_2 partial pressure (Ananad et al., 1995; Siriwardane et al., 2001). Van der Vaart et al. (1999) investigated the single and mixed gas adsorption equilibrium of CO_2/CH_4 on Norit RBI activated carbon. The CO_2 adsorption capacity was 108 mg/g-adsorbent at 21.5°C. With increasing temperature, the adsorption capacity decreased to 77 mg/g-adsorbent at 30°C, 56 mg/g-adsorbent at 56°C, and 40 mg/g-adsorbent at 75°C. Meanwhile, the activated carbon also adsorbed methane. The CO_2/CH_4 selectivity was around 2. Berlier et al. (1997) and Heuchel et al. (1999) also found that

CO_2 adsorption capacity of activated carbon decreased significantly when the temperature slightly increased and the CO_2/CH_4 selectivity was low. Under 0.1 MPa CO_2 partial pressure, the adsorption capacity was 126 mg/g-adsorbent at 15°C and 78 mg/g-adsorbent at 45°C. The best CO_2/CH_4 ratio (selectivity) was around 2. Since all the gases are physically adsorbed into/onto these carbon and zeolite adsorbents, the separation factors (e.g., CO_2/N_2 ratio) are low. In order to operate at relatively high temperature and reach high separation selectivity, chemical adsorption has been studied. Unfortunately, the adsorbents only show a low CO_2 adsorption capacity at high temperature although the selectivity for CO_2 is high. Anand et al. (1995) reported that MgO showed an adsorption capacity of 8.8 mg/g-adsorbent at 400°C. Ding et al. (2000) investigated the adsorption performance of hydrotalcite and this material showed a CO_2 adsorption capacity of 22 mg/g-adsorbent at 400°C and 0.2 atm CO_2 partial pressure. Both types of adsorbents need high temperature operation and have a low adsorption capacity, thus they are not suitable for practical use for CO_2 separation. For practical applications, selective adsorbents with high capacity are desired. Many of the separations should preferably be operated at elevated temperature, e.g., higher than room temperature and up to ≈150°C for the flue gas of power plants. Developing an adsorbent with high CO_2 selectivity and high CO_2 adsorption capacity, which can also be operated at elevated temperature, is desired for more efficient CO_2 separation by the adsorption approach.

A new concept called "molecular basket", was investigated to develop a high-capacity, highly-selective CO_2 adsorbent (Xu, et al, 2002a,b; Xu et al., 2003). The proposed CO_2 "molecular basket" adsorbents can selectively "pack" CO_2 in condensed form in the mesoporous molecular sieve "basket" and therefore show high CO_2 adsorption capacity and high CO_2 selectivity. To make the "molecular basket' adsorbent and to capture a large amount of CO_2 gas, the adsorbent needs to have large-pore volume channels to serve as the "basket". In order to make the "basket" be a CO_2 "molecular basket", a substance with numerous CO_2-affinity sites is loaded into the pores of the support to increase the affinity between the adsorbent and CO_2 and, therefore, to increase the CO_2 adsorption selectivity and CO_2 adsorption capacity. In addition, the adsorption affinity to CO_2 by the CO_2-philic substance increased in the confined mesoporous environment and therefore the mesoporous molecular sieve can have a synergetic effect on the adsorption of CO_2 by the CO_2-philic substance. In the current investigation, the mesoporous molecular sieve MCM-41, which has a large pore volume, was selected as the "basket". The

sterically-branched polymer polyethylenimine (PEI), which has branched chains with numerous CO_2-capturing amino groups, was immobilized into the channels of the mesoporous molecular sieve. Branched amines have lower heat of adsorption than that of the primary amines, and thus desorption can be easier and requires less energy. The novel CO_2 "molecular basket" adsorbents were applied in the separation of CO_2 from simulated flue gases and boiler flue gases.

3.4.1 Experimental

3.4.1.1 Preparation of the Adsorbents

Mesoporous molecular sieve MCM-41 was hydrothermally synthesized from a mixture with the following composition: xAl_2O_3:$50SiO_2$:$4.32Na_2O$:$2.19(TMA)_2O$: 15.62(CTMA)Br:$3165H_2O$ (x=0, 0.05, 0.25). The synthesis procedure was established at Penn State (Reddy and Song, 1996), and is based on the method invented by researchers at Mobil (Beck et al., 1992). Cab-O-Sil fumed silica (Cabot Corporation), tetramethylammonium silicate solution (0.5 TMA/SiO_2, 10 wt.% SiO_2, Sachem Inc.), sodium silicate (containing 14 wt.% NaOH and 27 wt.% SiO_2, Aldrich), cetyltrimethyl-ammonium bromide [(CTMA)Br, Aldrich], aluminum isopropoxide (Aldrich) and deionized water were used as raw materials. The synthesis was carried out at 100°C for 40 h. After the synthesis, the solid product was recovered by filtration, washed several times with deionined water, dried at 100°C overnight and calcined at 550°C for 5 h to remove the template.

The polyethylenimine (PEI) modified MCM-41 was prepared by a wet impregnation method. In a typical preparation, the desired amount of PEI (viscous liquid) was dissolved in 8 g methanol while stirring for about 15 min, after which 2 g calcined MCM-41 was added to the PEI/methanol solution. The resultant slurry was continuously stirred for about 30 min. Then the slurry was dried at 70°C for 16 h under reduced pressure (700 mmHg). The as-prepared adsorbent was denoted as MCM-41-PEI-X, where X represents the loading of PEI as weight percentage in the sample. Different adsorbents were prepared by changing the preparation conditions, such as PEI loadings, preparation methods, preparation procedures, types of solvents, solvent/MCM-41 ratios, Si/Al ratios of MCM-41, and adding additives of polyethylene glycol (PEG). In one adsorbent, commercially available silica gel (SiO_2) (Merck, surface area 550 m^2/g) was used as the support instead of MCM-41. Details on the adsorbents and their corresponding preparation conditions are summarized in Table 3.4.1.

Table 3.4.1 Preparation Conditions and the Adsorption/Desorption Performance of the Adsorbents

Sample Name	Si/Al of MCM-41	PEI loading (wt %)	Solvent	Solution/MCM -41weight ratio	Adsorption Capacity[a] (mg CO_2/g-adsorbent)	Desorption capacity (%)
Si-MCM-41	Pure silica	---	---	---	8.6	103
Al-MCM-41-100	100	---	---	---	7.6	101
Al-MCM-41-500	500	---	---	---	7.5	100
Si-MCM-41-PEI-5	Pure silica	5	Methanol	4:1	7.7	105
Si-MCM-41-PEI-15	Pure silica	15	Methanol	4:1	19.4	103
Si-MCM-41-PEI-30	Pure silica	30	Methanol	4:1	68.7	98
Si-MCM-41-PEI-50	Pure silica	50	Methanol	4:1	112	99
Si-MCM-41-PEI-75	Pure silica	75	Methanol	4:1	133	101
Si-MCM-41-PEI-25-25[b]	Pure silica	50	Methanol	4:1	96.8	97
Al-MCM-41-100-PEI-50	100	50	Methanol	4:1	127	100
Al-MCM-41-500-PEI-50	500	50	Methanol	4:1	121	99
Si-MCM-41-PEI-50-H_2O	Pure silica	50	Water	4:1	111	100
PEI-30-Si-MCM-41[c]	Pure silica	30	Methanol	4:1	65.7	99
Si-MCM-41-PEI-50-M[d]	Pure silica	50	---	--	99	97
Si-MCM-41-PEI-50-S2	Pure silica	50	Methanol	2:1	97	98
Si-MCM-41-PEI-50-S8	Pure silica	50	Methanol	8:1	126	99
Si-MCM-41-PEI-30-PEG-20[e]	Pure silica	30	Methanol	4:1	77.1	100
SilicaGel-PEI-50[f]	---	50	Methanol	4:1	78.0	98
PEI	---	100	---	---	109	56

[a] The adsorption capacity was measured by TGA under pure CO_2 atmosphere at a flow rate of 100 ml/min at 75°C.

[b] The adsorbent was prepared by two-step impregnation method. In each step, 25 wt % PEI was loaded.

[c] The adsorbent was prepared by adding the PEI/methanol solution to the MCM-41 powder.

[d] The adsorbent was prepared by mechanical mixing method.

[e] PEG was added to the adsorbent of MCM-41-PEI-30. The weight percentage of PEG was 20 wt%.

[f] Silica Gel was used as support material, instead of MCM-41.

3.4.1.2 Characterization of the Adsorbents

The mesoporous molecular sieve MCM-41, before and after modification, and before and after adsorption separation, was characterized by X-ray diffraction (XRD) and N_2 adsorption/desorption. The XRD patterns were obtained on a Rigaku Geigerflex using Cu K_α radiation. The N_2 adsorption/desorption was carried out on a Quantachrome Autosorb 1 automated adsorption apparatus, from which the BET surface area, the pore volume and the pore size were obtained. The sample was out-gassed at 75°C for 48 h on a high vacuum line prior to adsorption. The pore volume of the mesoporous molecular sieve was calculated from the adsorbed nitrogen after complete pore condensation (P/P_0=0.995) using the ratio of the densities of liquid and gaseous nitrogen. The pore size was calculated by using the BJH method. The thermal chemical and physical properties of MCM-41, PEI and MCM-41-PEI were characterized by thermal gravimetric analysis (TGA). The TGA was performed on a PE-TGA 7 thermal gravimeter. About 10 mg of the sample was heated at 10°C/min to 600°C in airflow (100 ml/min).

3.4.1.3 Measurement of the CO_2 Adsorption/Desorption Performance

The adsorption and desorption performance of the adsorbent was measured using a PE-TGA 7 analyzer. The weight change of the adsorbent was used to determine the adsorption and the desorption performance. In a typical adsorption/desorption process, about 10 mg of the adsorbent was placed in a small sample cell, heated up to 100°C in a N_2 atmosphere at a flow rate of 100 ml/min, and held at that temperature (about 30 minutes) until there was no loss in weight. Then the temperature was decreased to the desired temperature and the 99.8 % bone-dry CO_2 adsorbate was introduced at a flow rate of 100 ml/min. In one experiment CO_2/N_2 gas mixtures were also used. After the adsorption, the gas was switched to 99.995% pure N_2 at a flow rate of 100 ml/min to perform desorption at the same temperature. The time for both the adsorption and desorption was 150 minutes. Adsorption capacity in mg of adsorbate/g-adsorbent and desorption capacity in percentage were used to characterize the adsorbent and were calculated from the weight change of the sample in the adsorption/desorption process. Desorption capacity in percentage was defined as the ratio of the amount of the gas desorbed over the amount of gas adsorbed. The impact of adsorption/desorption temperature and the CO_2

concentration in the adsorbate on the adsorption and desorption performance of the adsorbent was studied.

3.4.1.4 Adsorption Separation of Simulated Flue Gas Mixture

A gas mixture containing 14.9% CO_2, 4.25% O_2 and 80.85% N_2 was used as the adsorbate. In some experiments, the gas mixture was mixed with 10% moisture and used as the adsorbate.

The adsorption separation was carried out in a mobile flow adsorption system as shown in Figure 3.4.1. In a typical adsorption/desorption run, about 2.0 g of the powder adsorbent was placed in a stainless steel adsorption column (O.D., 1/2'; I.D., 3/8'), heated to 100°C in a helium atmosphere at a flow of 50 ml/min and held at that temperature overnight to ensure that there was no carbon dioxide or moisture adsorbed. The temperature was then decreased to 75°C and the dry or moist CO_2+N_2+O_2 gas mixture was introduced at 10 ml/min. Generally, the adsorption was carried out for 120 minutes. After the adsorption, the gas was switched to pure helium at a flow rate of 50 ml/min to perform the desorption at the same temperature. The time for desorption was 300 minutes. The flow rate of the effluent gas was measured by a soap-film flowmeter. The concentration of the effluent gas was measured on-line using a SRI 8610 C Gas Chromatography (GC) with TCD detector. The analysis was carried out every 5 minutes when the dry CO_2+N_2+O_2 gas mixture was used as the adsorbate and every 15 minutes when the moist CO_2+N_2+O_2 gas mixture was used as the adsorbate. Adsorption capacity in ml (STP) of adsorbate/g adsorbent and desorption capacity in percentage were used to characterize the adsorbent. The adsorption/desorption capacity was calculated from mass balance before and after the adsorption. The separation factor was defined as the mole ratio of the gases adsorbed over the mole ratio of the gases in the feed.

3.4.1.5 Adsorption Separation of a Boiler Flue Gas Mixture

The adsorption separation of CO_2 from boiler flue gases was investigated. Both natural gas-fired and coal-fired flue gases were used as feed gas. The composition of the natural gas-fired flue gas mixture was 7.4-7.7% CO_2, ~ 4.45% O_2, 200-300 ppm CO, 60-70 ppm NO_x, 14.6% H_2O and 73-74% N_2. The composition of the coal-fired flue gas mixture was 12.5-12.8% CO_2,

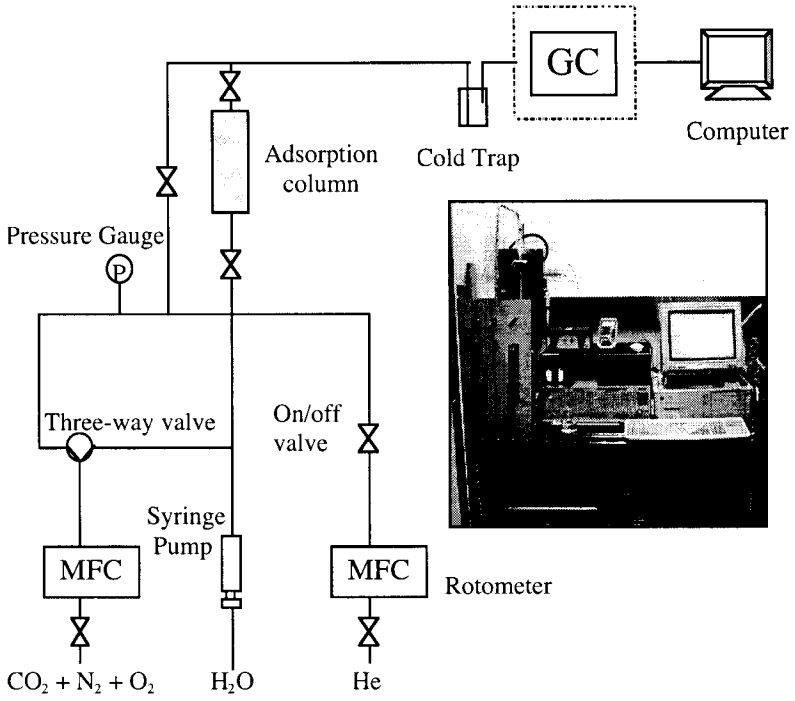

Figure 3.4.1 SET-UP OF THE ON-LINE CO_2 MONITORING SYSTEM

~4.4% O_2, 50 ppm CO, 420 ppm NO_x, 420 ppm SO_2, 6.2% H_2O and 76-77% N_2. Analysis of the effluent gas composition was carried out after removing water vapor from the gas mixture.

In a typical adsorption/desorption process, about 30 g of the adsorbent was placed in the central part of a stainless steel adsorption column (O.D., 2'; I.D., 1.7'). The adsorbent was pressed to 18-35 mesh. The beginning and the end of the adsorption column were filled with alumina (≈170 g) to decrease the dead volume in the separation system. The adsorption column was heated to 100°C in a helium atmosphere at a flow of 5 l/min and held at that temperature until there was no carbon dioxide detected in the effluent gas. The temperature was then adjusted to 80±10°C and the flue gas mixture was introduced at 5-6 l/min. Generally, the adsorption was carried out for 300-600 seconds. After the adsorption, the gas was switched to helium at a flow rate of 5 l/min to perform the desorption at the same temperature. The time for desorption was 300-600 seconds. The flow rate of the effluent gas was measured by a rotameter. The concentration of O_2, CO, CO_2, SO_2 and NO_x in the effluent gas was measured on-line using a model NGA 2000 paramagnetic oxygen analyzer; a model NGA 2000 non-dispersive infrared CO analyzer; a model NGA 2000 non-dispersive infrared CO_2 analyzer; a model 890 ultraviolet

SO_2 analyzer; and a model NGA 2000 chemiluminescence NO_x analyzer (Rosemount Analytical, Inc.), respectively. The analysis was carried out every 5-6 seconds. Since the alumina also adsorbed the gases, a blank separation test with the column filled with alumina (≈210 g) was carried out. Therefore, the adsorption/desorption capacity of the "molecular basket" adsorbent was calculated as the difference between the adsorption/desorption capacity from the adsorption experiment and blank experiment. The adsorption/desorption capacity was calculated from mass balance before and after the adsorption. The separation factor was defined as the mole ratio of the gases adsorbed over the mole ratio of the gases in the feed.

3.4.2 Results and Discussion

3.4.2.1 Preparation of the CO_2 "Molecular Basket" Adsorbent

Preparation and Characterization of the CO_2 "Molecular Basket" Adsorbent

Si-MCM-41-PEI with different PEI loadings was prepared and characterized by XRD, N_2 adsorption/desorption and TGA. Figure 3.4.2 shows the XRD patterns of Si-MCM-41 and Si-MCM-41-PEI with different PEI loadings. From comparing the diffraction patterns of Si-MCM-41 with those of Si-MCM-41-PEI with different PEI loadings, the degrees of the Bragg diffraction angles were nearly identical, indicating that the structure of Si-MCM-41 was preserved after loading the PEI. However, the intensity of the diffraction patterns of Si-MCM-41 decreased after the PEI was loaded. With increasing PEI loadings, the intensity of the diffraction peaks decreased. The intensity of the diffraction peaks of Si-MCM-41-PEI-50 and Si-MCM-41-PEI-75 were only 11% of that of the Si-MCM-41 support. At the same time, the degree of the Bragg diffraction angle of the 100 plane slightly increased from 2.265 for Si-MCM-41 to 2.295~2.325 for Si-MCM-41-PEI. These changes were possibly caused by the pore filling effect of the MCM-41 channels and the PEI coating on the outer surface of the MCM-41 crystals. Reddy and Song (1996) reported that the XRD patterns of MCM-41, after removal of the template, exhibited peaks with increased intensity and a shift to lower Bragg diffraction angle compared to the template-containing MCM-41. Since the pore volume of the Si-MCM-41 support is 1.0 ml/g and the density of PEI is about 1.0 g/ml, the maximum PEI loading in the pores of Si-MCM-41 is 50 wt %. More PEI should be coated on the outer surface of Si-MCM-

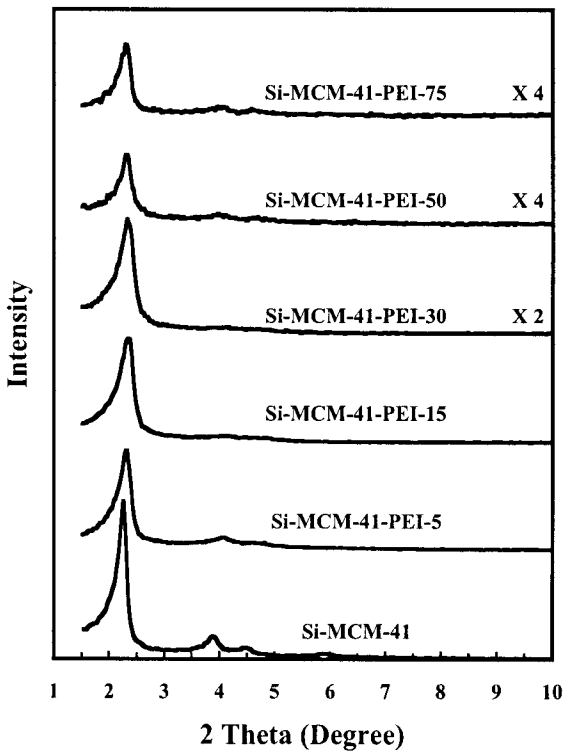

Figure 3.4.2 XRD PATTERNS OF Si-MCM-41-PEI WITH DIFFERENT PEI LOADINGS AS SHOWN BY THE TRAILING DIGITS (The top three curves were shown at different Y-scales.)

41 crystals for Si-MCM-41-PEI-75 than for Si-MCM-41-PEI-50. However, the diffraction intensity of Si-MCM-41 for Si-MCM-41-PEI-50 and Si-MCM-41-PEI-75 was nearly the same, which indicated that the PEI coating on the outer surface of the crystals hardly influenced the diffraction intensity of the Si-MCM-41 support. Therefore, the decrease in the diffraction intensity and the shift of the Bragg diffraction angle of the 100 plane to a high degree can be ascribed mainly to the loading of PEI into the Si-MCM-41's pore channels.

The pore size, surface area and pore volume of Si-MCM-41 before and after loading the PEI were obtained from the nitrogen adsorption/desorption isotherms. Figure 3.4.3 shows the pore size distributions of Si-MCM-41-PEI with different PEI loadings and Figure 3.4.4 shows their surface areas and pore volumes. The pore size of the Si-MCM-41 support was 2.75 nm. After the PEI was loaded into its channels, the pore size decreased. The pore size of Si-MCM-41-PEI-5 was 2.47 nm, smaller than that of the Si-MCM-41 support, which confirmed that PEI was loaded into the Si-MCM-41 pore channels. With increasing PEI loading, the pore size

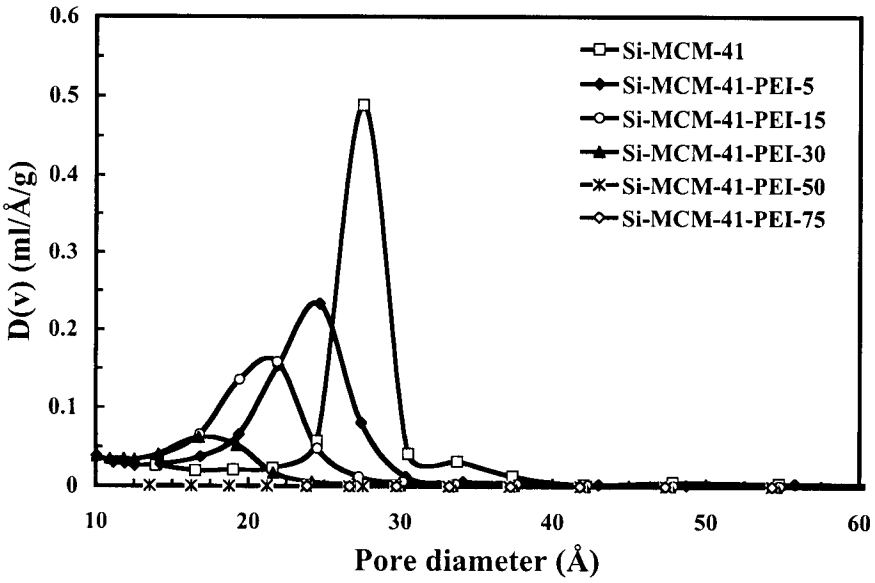

Figure 3.4.3 THE PORE SIZE DISTRIBUTION OF Si-MCM-41-PEI WITH DIFFERENT PEI LOADINGS

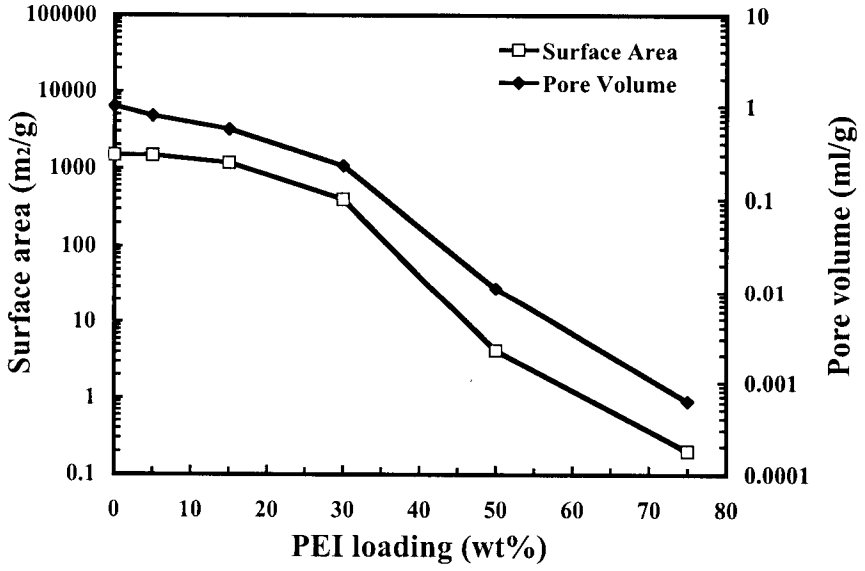

Figure 3.4.4 THE SURFACE AREA AND PORE VOLUME OF Si-MCM-41-PEI WITH DIFFERENT PEI LOADINGS

further decreased. The pore sizes were 2.19 nm and 1.68 nm for Si-MCM-41-PEI-15 and Si-MCM-41-PEI-30, respectively. When the PEI loading was further increased to 50 wt %, the mesoporous pore channels were completely filled with PEI, restricting the access of nitrogen into the pores at the liquid nitrogen temperature. Therefore, information on the pore size cannot be obtained from the N_2 adsorption/desorption isotherms for PEI loadings above 50 wt %. This is also consistent with the estimated maximum PEI loading of 50 wt % inside the pores of Si-MCM-41 (based on the pore volume of the Si-MCM-41 and the density of PEI).

The surface area and the pore volume of Si-MCM-41, after loading the PEI, exhibited the same trends as the pore size. The Si-MCM-41 support had a surface area of 1,486 m^2/g and a pore volume of 1.0 ml/g. The surface area and the pore volume decreased after PEI was loaded into its channels. For example, when the PEI loading was 5.0 wt %, the adsorbent showed a pore volume of 0.79 ml/g, smaller than that of the Si-MCM-41 support, which confirmed that PEI was loaded into the Si-MCM-41's channels. With increasing PEI loadings, the surface area and the pore volume further decreased. When the PEI loading was higher than 30 wt %, the surface area decreased sharply, which indicated that some of the mesoporous pores were completely filled with PEI. The surface area was only 4.2 m^2/g and the residual pore volume was only 0.011 ml/g for Si-MCM-41-PEI-50 at the liquid nitrogen temperature. These results correlate with the pore filling effect of the PEI, which was also evident from the XRD characterization, and further confirms that PEI was loaded into the pore channels of Si-MCM-41.

The thermal chemical and physical properties of Si-MCM-41, PEI and Si-MCM-41-PEI were measured by TGA. Figure 3.4.5 shows the TGA results and Figure 3.4.6 shows the differential thermal gravimetric analysis (DTGA) results. As expected, there was no weight loss for Si-MCM-41 below 600°C, which indicated that the hydrophobic Si-MCM-41 was free from adsorbed water or other gases at room temperature. The PEI lost 3.8% of its original mass at 100°C, which can be mainly ascribed to the desorption of CO_2 and moisture. This was confirmed by analyzing the effluent gas with a gas chromatograph (GC). This also indicated that PEI has a low vapor pressure and unlike the commercially used amines such as diethanolamine (DEA), makes PEI suitable for long-term use at relatively high temperature. The PEI began to decompose above 150°C and a sharp weight loss appeared at 205°C. When the temperature was increased above 225°C, the rate of weight loss decreased, indicating that a different decomposition process took place. At 600°C, the PEI was completely decomposed and removed

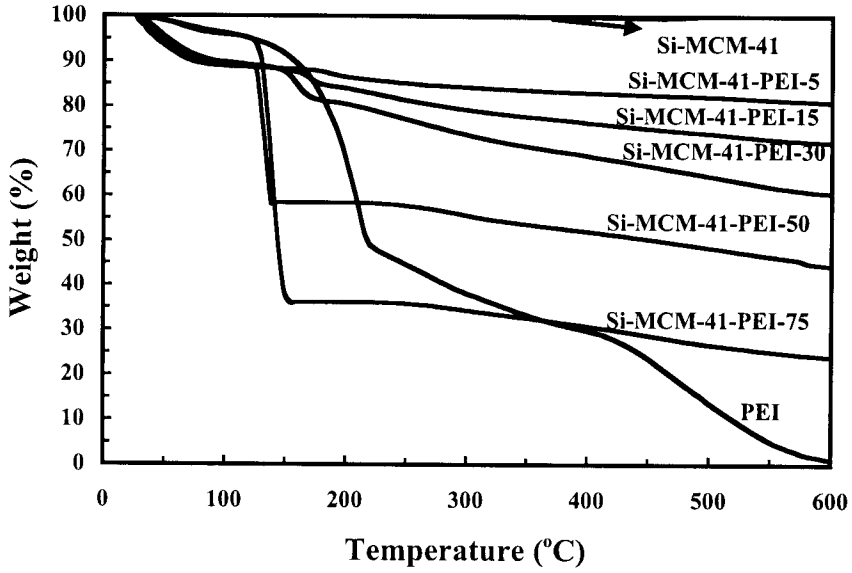

Figure 3.4.5 TGA PROFILE FOR Si-MCM-41-PEI WITH DIFFERENT LOADINGS

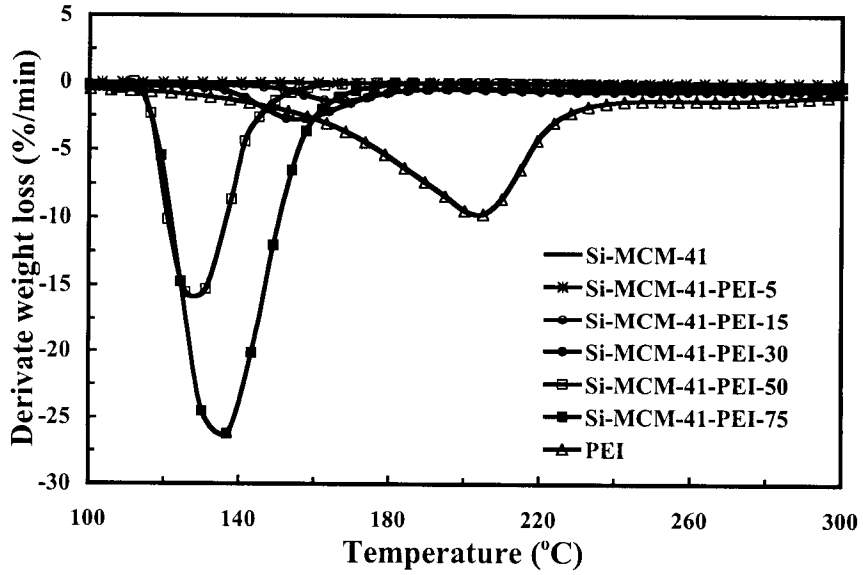

Figure 3.4.6 DTGA PROFILE FOR Si-MCM-41-PEI WITH DIFFERENT PEI LOADINGS

as volatiles. After the PEI was loaded into the Si-MCM-41's channels, the sharp weight loss of the PEI took place at a lower temperature, which indicated that the decomposition temperature of PEI decreased. The weight loss also took place over a narrower temperature range than that of the pure PEI. These phenomena can be explained by the uniform dispersion of PEI into the nano-porous support pores, since the melt or decomposition temperature will decrease when the particle size of a substance decreases (Zeng, et al., 1998). In addition, when the PEI loading was below 50 wt %, Si-MCM-41-PEI showed a ~10.5% weight loss at 100°C, which was higher than that of the pure PEI and can be ascribed also to desorption of CO_2 and moisture. When the PEI loading was 75 wt %, the weight loss was only ≈3.5% at 100°C, similar with that of the pure PEI, which indicated that PEI was coated on the outer surface of the molecular sieve crystals and the composite material behaved like the pure PEI particles. The different weight losses observed at 100°C, between the Si-MCM-41-PEI-50 and Si-MCM-41-PEI-75, further confirmed that the PEI was loaded into the MCM-41's channels. The weight loss of Si-MCM-41-PEI also indicated that there was no PEI loss during the preparation process. For example, the total weight loss for Si-MCM-41-PEI-50 was ~56% at 600°C. If the adsorbed moisture or CO_2 is excluded from the total weight loss, then the PEI loading is calculated to be about 50 wt %, which is in accordance with the designed PEI loading.

Adsorption Performance of MCM-41-PEI

The Influence of Operating Temperature on CO_2 Adsorption

The adsorption and desorption performances of the MCM-41-PEI-50 at different temperatures in pure CO_2 atmosphere were measured and the results are shown in Figure 3.4.7. With increasing temperatures, the adsorption capacity of the MCM-41-PEI-50 increases and reaches its maximum of 112 mg/g adsorbent at 75°C. When the temperature was increased to 100°C, the adsorption capacity slightly decreased to 110 mg/g adsorbent. The desorption was not complete at low temperature. When the temperature was 50°C, about 20% of the CO_2 desorbed. The desorption was complete when the temperature reached 75°C. However, the desorption capacity decreased when the temperature was 100°C.

The adsorption of CO_2 into PEI or MCM-41 is an exothermic process (Kohl and Nielson, 1997). Accordingly, the adsorption capacity should decrease with increasing temperature. However, the adsorption capacity increased with increasing temperature in this study. At low

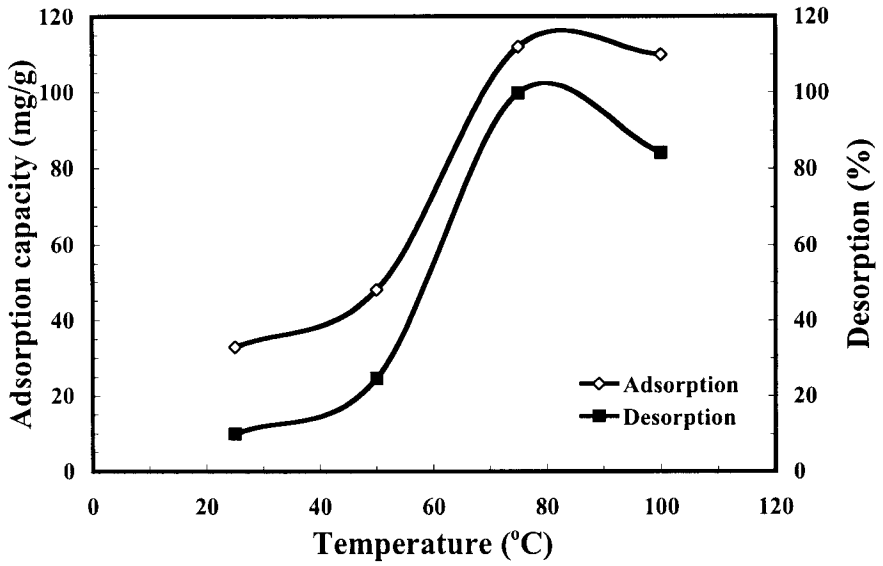

Figure 3.4.7 THE INFLUENCE OF OPERATING TEMPERATURE ON THE ADSORPTION AND DESORPTION PERFORMANCE OF Si-MCM-41-PEI-50

temperature, the PEI exists in the channels of MCM-41 like nano-sized particles. In this case, only the CO_2 affinity sites on the surface of the particles can readily react with CO_2. The affinity sites inside the nano-sized particles can only react with CO_2 when the CO_2 has diffused into the particles. This is a kinetically (diffusion)-controlled process, since the access of CO_2 to the affinity sites inside the PEI particles will be subject to the diffusion limitation, and CO_2 may reach more affinity sites if the diffusion time is sufficiently long. In this case, more affinity sites will be exposed to the CO_2 and thus the adsorption capacity will increase when using a short adsorption time.

In order to verify the above hypothesis, the following experiment was designed. First, the adsorption of CO_2 was carried out at 75°C in flowing CO_2 for 150 min, the temperature was then decreased to 25°C and held at that temperature for another 150 min. If the adsorption capacity increased at low temperature, it can be concluded that the low adsorption capacity at low temperature was caused by the kinetic limitation. If the adsorption capacity decreased, other reasons may cause the low adsorption capacity at low temperature. The experimental results are shown in Figure 3.4.8. The adsorption capacity was 110 mg/g-adsorbent at 75°C. When the temperature was decreased to 25°C and held for 150 min, the adsorption capacity increased to

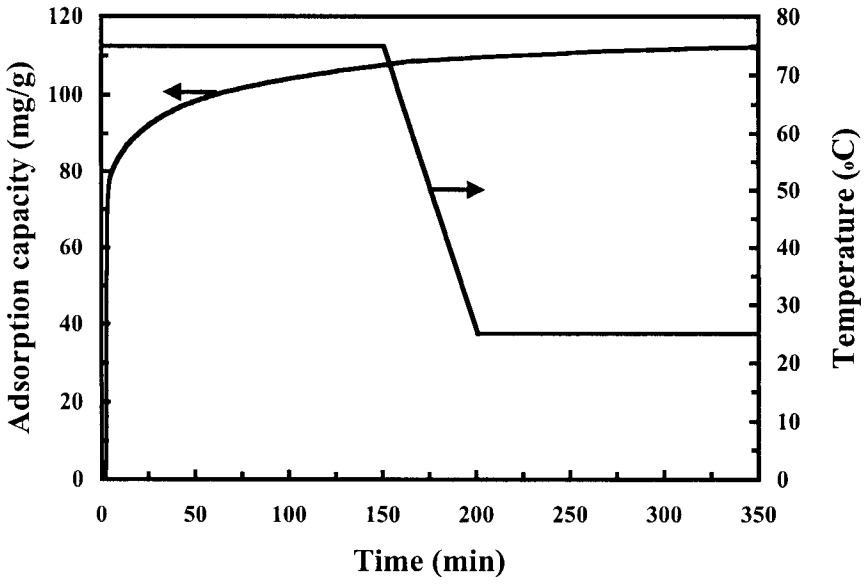

Figure 3.4.8 TEMPERATURE PROGRAMMED ADSORPTION OF CO_2 BY Si-MCM-41-PEI-50 (Pure CO_2 atmosphere, CO_2 flow rate: 100 ml/min)

112 mg/g adsorbent, which means that the adsorption is kinetically controlled. The low adsorption capacity at low temperature is therefore a result from the low adsorption rate. The adsorption capacity at low temperature will be larger than that at high temperature if the adsorption time is long enough to ensure that equilibrium is attained.

The Influence of CO_2 Concentration on CO_2 Adsorption

Because the concentration of CO_2 varies in different gas mixtures, from about 13% in flue gas from coal-fired power plants to about 0.6% in space vehicles (Satyapal et al., 1973), the influence of CO_2 concentration in a CO_2/N_2 gas mixture on the adsorption and desorption performance of MCM-41-PEI-50 was investigated at 75°C. The results are shown in Figure 3.4.9. Since the adsorption of N_2 is negligible in the presence of CO_2, the adsorption amount measured for the CO_2/N_2 mixture was considered to be the CO_2 adsorption capacity. For pure CO_2, the adsorption capacity was 112 mg/g adsorbent. With a decrease in the CO_2 concentration, the adsorption capacity of the MCM-41-PEI-50 also decreased somewhat. When the CO_2 concentration in the feed decreased to 30%, the adsorption capacity decreased to 102

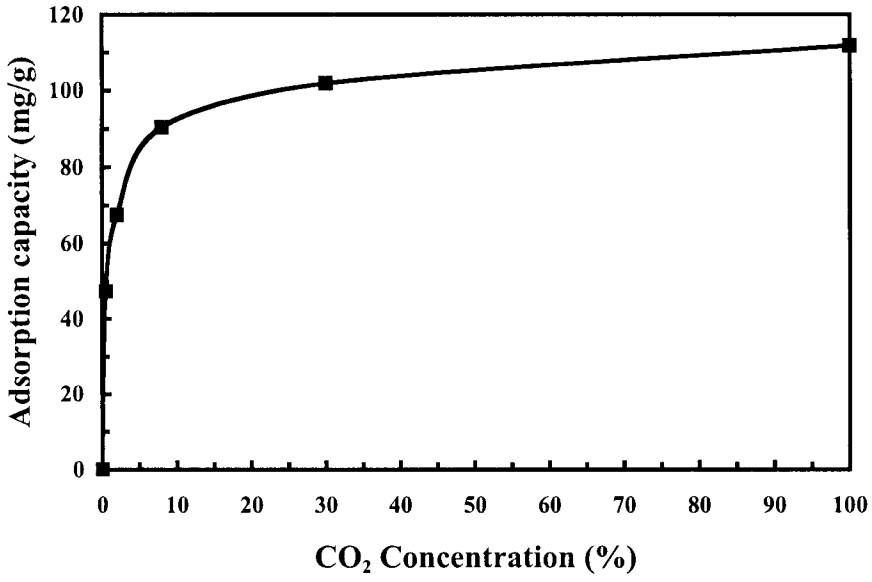

Figure 3.4.9 THE INFLUENCE OF CO_2 CONCENTRATION IN THE CO_2/N_2 MIXTURE ON THE ADSORPTION PERFORMANCE OF Si-MCM-41-PEI-50 (Operating temperature 75°C, flow rate 100 ml/min)

mg/g adsorbent and was about 9% lower than that in the pure CO_2 atmosphere. When the CO_2 concentration was further decreased to 8% and 2%, the adsorption capacities decreased to 90.4 and 67.5 mg/g respectively. Even when the CO_2 concentration was 0.5% (i.e., 3.8 mmHg), the MCM-41-PEI-50 still effectively captured CO_2 from the gas mixture. The adsorption capacity was 47.6 mg/g adsorbent at a CO_2 concentration of 0.5%. The desorption of the CO_2 was complete over the CO_2 concentration range investigated.

The main reaction responsible for CO_2 interaction with amine (chemical adsorption) is believed to be carbamate formation:

$$CO_2 + 2R_2NH = R_2NH_2^+ + R_2NCOO^-$$

Since the experiment was carried out in a flow system, the amount of CO_2 was in significant excess. However, the adsorption capacity was related to the CO_2 concentration in the gas mixture at a given temperature, which implied that the reaction was partially thermodynamically controlled. In order to increase the adsorption capacity, the partial pressure of the CO_2 must be increased. But the experimental data showed that the adsorption capacity seems to be related to the logarithm of the CO_2 pressure. Increasing the CO_2 pressure will lead to less increase in the

adsorption capacity and may increase the operating cost. The other optional way is to make MCM-41-PEI materials in a membrane form. In this case, the reaction (chemical adsorption) will occur at the feed side and the inverse reaction (desorption after chemisorption) will occur at the permeate side. Thus, the CO_2 can be recovered. In addition, the separation can be operated continuously.

The Influence of Preparation Conditions on the Adsorption Performance of MCM-41-PEI

The Effect of PEI Loadings on CO_2 Adsorption

The influence of PEI loading on the CO_2 adsorption performance of Si-MCM-41-PEI was investigated in a pure CO_2 atmosphere at 75°C and the results are shown in Figure 3.4.10. Before the PEI was loaded, the Si-MCM-41 support alone showed a CO_2 adsorption capacity of 8.6 mg/g-adsorbent. The low adsorption capacity was caused by the weak interaction between CO_2 and Si-MCM-41 at relatively high temperature. In order to strengthen the interaction between CO_2 and Si-MCM-41, the branched polymeric substance PEI with numerous CO_2-capturing sites, was loaded into the Si-MCM-41 channels. Surprisingly, the PEI made no contribution to the CO_2 adsorption capacity at low PEI loading. When the PEI loading was 5.0 wt %, the CO_2 adsorption capacity was only 7.7 mg/g-adsorbent, nearly identical to that of the Si-MCM-41 support. When the PEI loading was further increased, the adsorption capacity increased. The adsorption capacities were 19 mg/g-adsorbent and 69 mg/g-adsorbent for PEI loadings of 15 wt % and 30 wt %, respectively. At 50 wt % PEI loading, the adsorption capacity was 112 mg/g-adsorbent, which is higher than that of the pure PEI of 110 mg/g-adsorbent. The mesoporous molecular sieve of Si-MCM-41 showed a synergetic effect on the adsorption of CO_2 by PEI. The highest adsorption capacity of 133 mg/g-adsorbent was obtained when the PEI loading was 75 wt %.

The desorption was complete for all the Si-MCM-41-PEI adsorbents as well as for the Si-MCM-41 support. However, the desorption for pure PEI was slow and was not complete in the desorption time of the Si-MCM-41-PEI absorbents. The fast desorption of CO_2 from the Si-MCM-41-PEI absorbents can be explained by the high dispersion of the PEI into the Si-MCM-41 channels as shown by the XRD, N_2 adsorption/desorption and TGA characterizations.

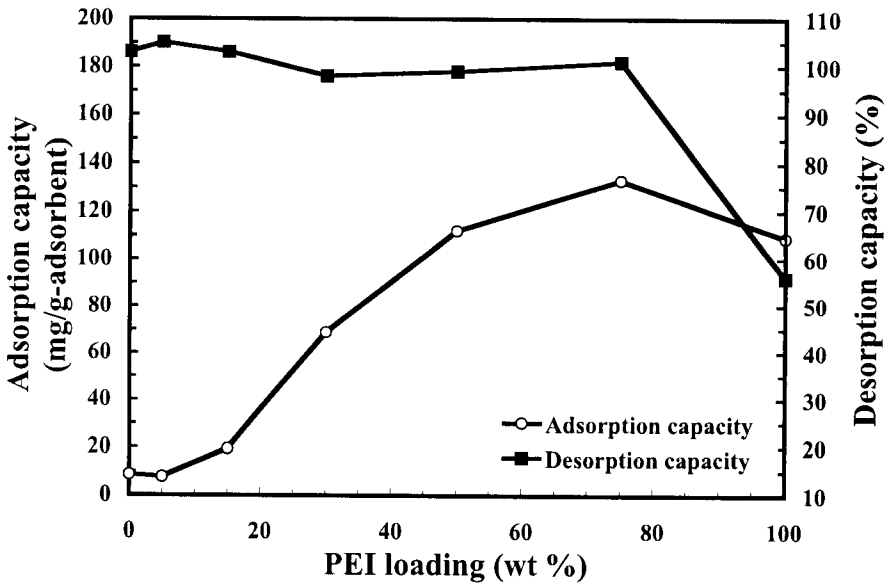

Figure 3.4.10 THE INFLUENCE OF PEI LOADINGS ON THE ADSORPTION AND DESORPTION PERFORMANCE OF Si-MCM-41-PEI

The Effect of Preparation Methods and Preparation Procedures on CO_2 Adsorption

Two methods, i.e., wet impregnation and mechanical mixing, were employed for the preparation of Si-MCM-41-PEI. For the mechanical mixing method, PEI was solidified, ground into powder and mixed uniformly with Si-MCM-41 at the liquid nitrogen temperature. The powder mixture was heated to 70°C and held at that temperature for 16 h under reduced pressure (700 mmHg). The PEI loading was 50 wt %. The adsorption performance of this absorbent was compared with that of the adsorbent prepared by the wet impregnation method in Table 3.4.1. The adsorption capacity was 99 mg/g-adsorbent for the adsorbent prepared by the mechanical mixing method (Si-MCM-41-PEI-50-M) and 112 mg/g-adsorbent for the adsorbent prepared by the wet impregnation method (Si-MCM-41-PEI-50). The adsorption capacity of Si-MCM-41-PEI-50-M was lower than that of Si-MCM-41-PEI-50. The higher adsorption capacity for the wet impregnation method was possibly caused by the uniform dispersion of PEI into the Si-MCM-41 channels. However, if the PEI and the Si-MCM-41 were simply mechanically mixed in Si-MCM-41-PEI-50-M, the adsorption capacity of MCM-41-PEI-50-M should be the linear sum of the adsorption capacities contributed by the Si-MCM-41 and PEI, and was calculated to be 58.9 mg/g-adsorbent. The adsorption capacity of Si-MCM-41-PEI-50-M was higher than this

value, which indicated that part of the PEI may also be loaded into the Si-MCM-41 channels or be coated on the external surface of the support crystals during the thermal treatment. The desorption for both of the adsorbents was complete.

In addition, two different impregnation procedures were examined. In the first set of experiments, the adsorbent was prepared by adding the PEI-methanol solution to Si-MCM-41 (PEI-30-Si-MCM-41). Its adsorption performance was compared with that of the adsorbent prepared by adding Si-MCM-41 to the PEI-methanol solution (Si-MCM-41-PEI-30) in Table 3.4.1. The adsorption/desorption capacities of these two adsorbents were similar, which indicates that the impregnation procedure did not influence the dispersion of PEI into the Si-MCM-41 channels nor the adsorption performance of the adsorbent.

In the second set of experiments, the adsorbent was prepared by the following procedure: Si-MCM-41 was first impregnated with 25 wt % PEI, then dried under vacuum at 70°C, and another 25 wt % PEI was then loaded. The adsorption performance of this adsorbent (Si-MCM-41-PEI-25-25) was compared with that of the adsorbent loaded with 50 wt % PEI in one step (Si-MCM-41-PEI-50) in Table 3.4.1. The adsorption capacity of Si-MCM-41-PEI-50 was higher than that of Si-MCM-41-PEI-25-25, which indicates that one-step impregnation is a better method than two-step impregnation. Since PEI is hydrophilic in nature, the PEI impregnated in the first step may adsorb the methanol and prevent the PEI from entering the MCM-41 channels in the next step of impregnation. Therefore, PEI may coat the external surface of the support crystals in the second impregnation and the adsorption capacity is decreased.

The Effect of Solvent Type and Methanol/MCM-41 Weight Ratio on CO_2 Adsorption

Since the Si-MCM-41 that was used was pure silica and was hydrophobic in nature, the polarity of the solvent for the dissolution of PEI may influence the dispersion of PEI into the Si-MCM-41 channels. Two solvents, i.e., methanol and water, were used to examine the effect of solvent on adsorbent performance. The PEI loading for both adsorbents was 50 wt % and the adsorption results are shown in Table 3.4.1. The adsorption capacity was nearly the same for the two adsorbents, which indicated that these two solvents had limited influence on the adsorption performance of the resulting adsorbent. The results also indicate that PEI is more hydrophobic than both water and methanol, and was therefore preferentially adsorbed into the Si-MCM-41 channels from the solution. Because methanol is easier to volatilize than water and the Si-MCM-

41 structure is not stable under a steam atmosphere at high temperature, methanol was selected as the solvent for the dissolution of PEI in the subsequent study.

The influence of the methanol/Si-MCM-41 weight ratio on the adsorption performance of the resultant adsorbents was also examined and the adsorption results are shown in Table 3.4.1. From the adsorption results, it can be concluded that the adsorption capacity increased with increasing methanol/Si-MCM-41 weight ratio. The highest adsorption capacity of 126 mg/g-adsorbent was obtained when the methanol/Si-MCM-41 weight ratio was 8, which was 23% higher than that of the adsorbent prepared with a methanol/Si-MCM-41 weight ratio of 2. When the methanol/Si-MCM-41 weight ratio was 2, the Si-MCM-41 cannot be wetted well by the PEI/methanol solution. In this case, the PEI cannot be dispersed well and the adsorption capacity was nearly equal to that of the adsorbent prepared by the mechanical mixing method. When the methanol/Si-MCM-41 weight ratio was increased to 4, MCM-41 can be wetted by the PEI/methanol solution, allowing more PEI to be loaded into the Si-MCM-41 channels and thus increasing the adsorption capacity.

The Effect of Polyethyleneglycol (PEG) as an Additive on CO_2 Adsorption

The influence of PEG on the adsorption performance of Si-MCM-41-PEI was investigated. Figure 3.4.11 compares the adsorption and desorption performance of Si-MCM-41-PEI-30 and Si-MCM-41-PEI-30-PEG-20. The CO_2 adsorption capacity and the CO_2 adsorption/desorption rate for Si-MCM-41-PEI changed after adding the PEG to Si-MCM-41-PEI. The adsorption capacity of Si-MCM-41-PEI-30-PEG-20 was higher than that of Si-MCM-41-PEI-30. In addition, the adsorption/desorption rates for Si-MCM-41-PEI-30-PEG-20 were faster than those for Si-MCM-41-PEI-30. Satyapal et al. (2001) also found that adding PEG to the PEI/polymer adsorbent can accelerate the CO_2 adsorption and desorption rates. The authors suggested that the enhancement of the adsorption and desorption rates was related to the preponderance of OH- ions from the PEG molecules. They also suggested that the PEG attracts more water to the adsorbent due to the hydroscopic nature of the chemical. Since the adsorbate was pure CO_2 in the current experiment and there was no moisture in the gas, the enhanced adsorption capacity in this study must emanate from the CO_2 alone.

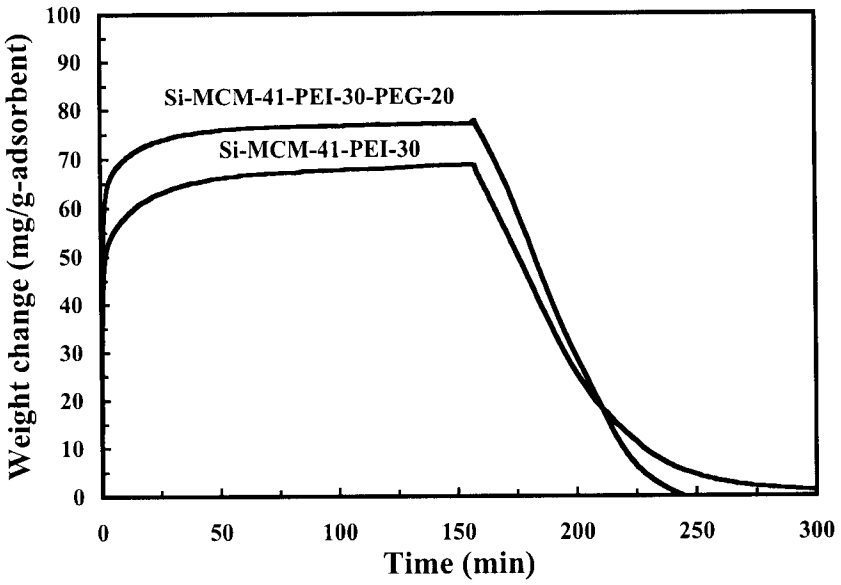

Figure 3.4.11 THE EFFECT OF PEI ON THE CO_2 ADSORPTION/DESORPTION PERFORMANCE OF Si-MCM-41-PEI (PEI loading: 30 wt %, PEG loading: 20 wt %)

The Effect of the Si/Al Ratio on the MCM-41 Support on CO_2 Adsorption

The above results were derived using pure silica of MCM-41. To clarify whether aluminum incorporation into MCM-41 framework can affect the property of the MCM-41-PEI adsorbent, the influence of the Si/Al ratio of the MCM-41 support on the adsorption performance of the resultant adsorbents was examined. Figure 3.4.12 shows the adsorption capacity of MCM-41 and MCM-41-PEI-50 with different support Si/Al ratios. The adsorption capacity was nearly identical for the MCM-41 support with different Si/Al ratios. However, the adsorption capacity of MCM-41-PEI was influenced by the Si/Al ratio of the MCM-41support. The lower the Si/Al ratio of the MCM-41 support, the higher the adsorption capacity of the resultant adsorbent. The adsorption capacity of Al-MCM-41-100-PEI-50 was 127 mg/g-adsorbent and was 12 % higher than that of Si-MCM-41-PEI-50.

The Effect of the "Molecular Basket" on CO_2 Adsorption

In order to reveal any synergetic effects between MCM-41 and PEI on CO_2 adsorption, the linear adsorption capacity and the synergetic adsorption gain were defined as follows:

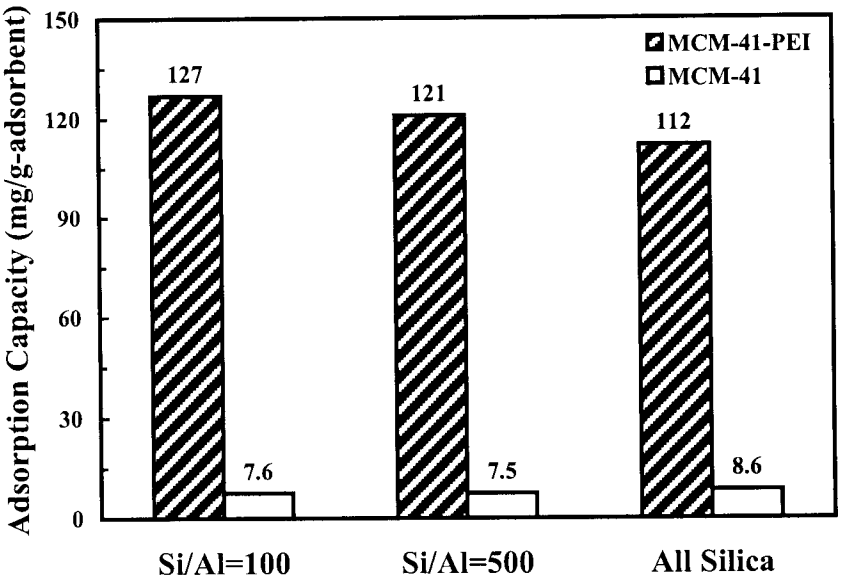

Figure 3.4.12 THE INFLUENCE OF Si/Al RATIO OF THE MCM-41 SUPPORT ON THE CO_2 ADSORPTION PERFORMANCE OF MCM-41 and MCM-41-PEI (PEI loading: 50 wt %)

Linear adsorption capacity (mg adsorbate/g-adsorbent) = [(MCM-41 weight percentage in the adsorbent × Adsorption capacity of pure MCM-41) + (PEI weight percentage in the adsorbent × Adsorption capacity of pure PEI)]

Synergetic adsorption gain (mg adsorbate/g-adsorbent) = Adsorption capacity of the adsorbent – Linear adsorption capacity

The linear adsorption capacity and the synergetic adsorption gain were calculated and are shown in Figure 3.4.13. For Si-MCM-41-PEI-5 and Si-MCM-41-PEI-15, the synergetic adsorption gain was close to zero, indicating that the loading of PEI into the Si-MCM-41 channels had no effect on the increase in the CO_2 adsorption capacity at these low PEI loadings. When the PEI loading was higher than 30 wt %, a synergetic adsorption gain was observed, which indicated that PEI modified Si-MCM-41 began to act as a CO_2 "molecular basket". The highest synergetic gain was obtained at a PEI loading of 50 wt %, while the synergetic adsorption gain decreased at the PEI loading of 75 wt %.

By correlating the adsorption performance and the pore structure of Si-MCM-41 and Si-MCM-41-PEI, a simple model was proposed in Figure 3.4.14 to account for the synergetic effect of Si-MCM-41 on CO_2 adsorption by PEI. Since the adsorption was operated at a relatively high temperature and the pore size of Si-MCM-41 is in the mesoporous region, the CO_2 adsorption

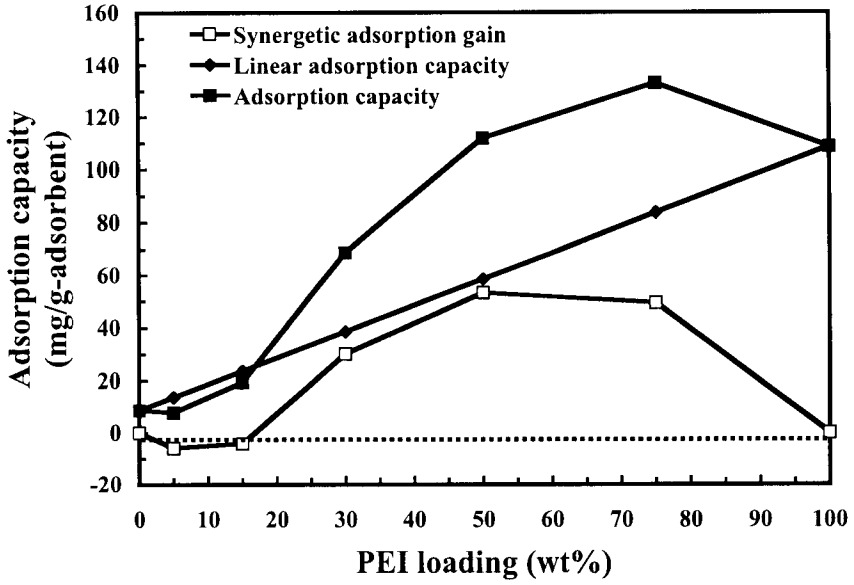

Figure 3.4.13 SYNERGETIC EFFECT OF Si-MCM-41 ON THE ADSORPTION OF PEI AS A FUNCTION OF PEI LOADING IN MCM-41-PEI

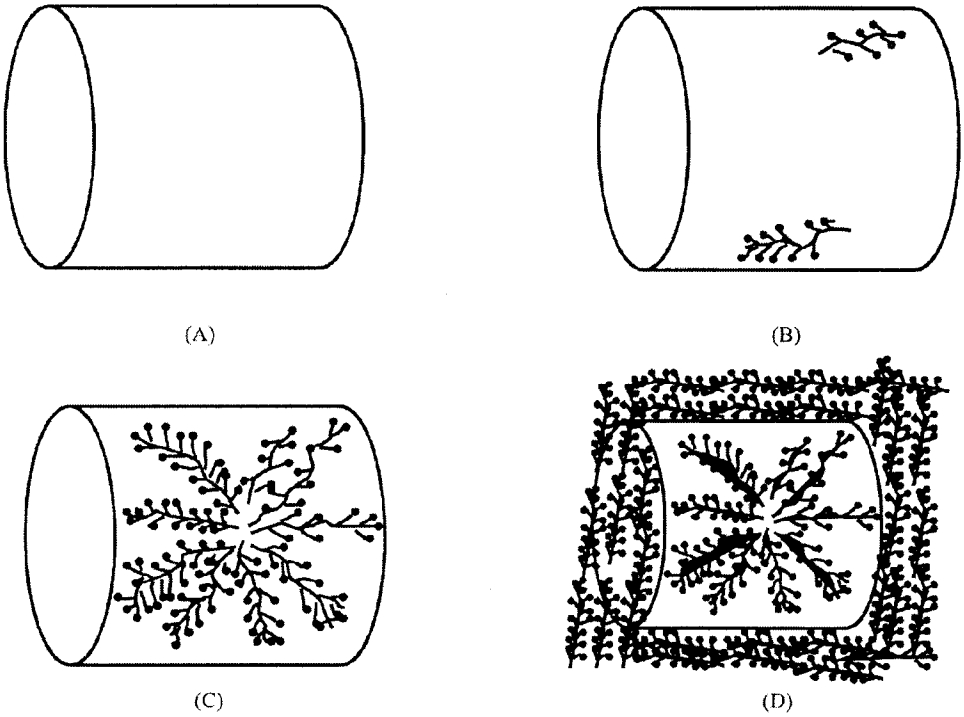

Figure 3.4.14 SCHEMATIC DIAGRAM OF PEI LOADED IN THE MESOPOROUS MOLECULAR SIEVE OF MCM-41 ((A) MCM-41 support; (B) Low PEI loading; (C) High PEI loading; (D) Extremely high PEI loading)

capacity of Si-MCM-41 alone is low. When the PEI, which has branched chains with numerous CO_2 adsorption sites of the amine group, is loaded into the Si-MCM-41 channels, both the physical adsorption by capillary condensation and the chemical adsorption by reaction with PEI will contribute to the adsorption capacity. It may be expected that the adsorption capacity of Si-MCM-41-PEI would increase with increasing amount of PEI loaded. However, only at high PEI loading did Si-MCM-41-PEI show a synergetic effect on CO_2 adsorption, indicating a strong interaction between Si-MCM-41 and PEI. When the PEI loading was low, the pore size of the adsorbent slightly decreased, from 2.75 nm for Si-MCM-41 to 2.47 nm for Si-MCM-41-PEI-5. In this case, the PEI was mostly adsorbed on the inner pore wall of the Si-MCM-41 support (Figure 3.4.14B). Both physical adsorption and chemical adsorption contribute to CO_2 uptake in this case. The adsorption capacity was even smaller than that of the linear adsorption capacity. With increasing PEI loadings, the pore size further decreased. At the same time, because more PEI was loaded into the channels, the chemical adsorption of CO_2 became much more dominant than that at low PEI loadings. The physical adsorption on the unmodified pore wall of Si-MCM-41 (and the capillary condensation in the mesopore) became negligible when compared to the chemical adsorption force. In addition, mesoporous molecular sieve Si-MCM-41 had a synergetic effect on the adsorption of CO_2 by PEI in the confined mesoporous pores (Xu et al., 2002a). Therefore, the CO_2 adsorption capacity increased. The highest synergetic adsorption gain (Figures 3.4.13 and 3.4.14C) was obtained when the mesoporous channels were completely filled with PEI, i.e., about 50 wt % of PEI loading. When the PEI loading further increased to 75 wt % (Figures 3.4.13 and 3.4.14D), the synergetic adsorption gain was smaller than that for the PEI loading of 50 wt %. Since the pore volume of Si-MCM-41 is about 1.0 ml/g and the density of PEI is about 1.0 g/ml, the largest amount of PEI that can be theoretically loaded into 1.0 g Si-MCM-41 is 1.0 ml, i.e., 50 wt % PEI loading. For the adsorbent with PEI loading of 75 wt %, theoretically, only one third of the PEI could be loaded into the Si-MCM-41 channels and two thirds of the PEI would be coated on the external surface of the molecular sieve particles. Interestingly, the highest adsorption gain (weighed on PEI) was also at the 50 wt % PEI loading, which indicated that only when the PEI was loaded into the mesoporous molecular sieve did the Si-MCM-41 and PEI show a strong synergetic effect on CO_2 adsorption. When the PEI was coated on the external surface of the molecular sieve crystals, the synergetic effect was limited. In order to distinguish the synergetic effect of the PEI in the mesoporous channels and on the

external surface of the molecular sieve crystals, the adsorption capacity of the PEI only in the "molecular basket" adsorbent was calculated as follows:

> **PEI adsorption capacity** (mg adsorbate/g-PEI) = [Adsorption capacity of the adsorbent –(MCM-41 weight percentage in the adsorbent × Adsorption capacity of pure MCM-41)]/ (PEI weight percentage in the adsorbent)

The calculated PEI adsorption capacity is 215 mg/g-PEI for Si-MCM-41-PEI-50 and 174 mg/g-PEI for Si-MCM-41-PEI-75. Since the Si-MCM-41-PEI-75 was prepared with 25 wt % of Si-MCM-41 and 75 wt % of PEI, it was assumed that 25 wt % of the PEI is loaded into the pores of the Si-MCM-41 and the other 50 wt % of the PEI is coated on the external surface of the Si-MCM-41. If it is assumed that the PEI loaded into the Si-MCM-41 channel shows the same adsorption capacity as that of the Si-MCM-41-PEI-50, the adsorption capacity of the PEI that was coated on the external surface of Si-MCM-41for Si-MCM-41-PEI-75 can be calculated and is found to be only154 mg/g-PEI. The adsorption capacity for the PEI coated on the external surface of the crystal was much lower than that of the Si-MCM-41-PEI-50 (215 mg/g-PEI) when the PEI was fully filled in the channels of the Si-MCM-41, which confirmed that only when the PEI was loaded into the channels of the mesoporous molecular sieve did the Si-MCM-41 exhibit the highest synergetic effect and proved that the "molecular basket" concept resulted in the significant improvement on the CO_2 adsorption by PEI.

The adsorption capacity for the PEI coated on the external surface of the crystal was slightly greater than that of the pure PEI of 110 mg/g-PEI. When the PEI was coated on the crystal surface, more adsorption sites will be exposed to the adsorbate. Therefore, the adsorption capacity will be higher than that of the bulk PEI. This can also be verified by the CO_2 adsorption capacity of PEI coated on other high-surface-area materials such as silica gel. When the PEI was coated on a high-surface-area silica gel (550 m^2/g) and the PEI loading was 50%, the CO_2 adsorption capacity was only 156 mg/g-PEI, slightly higher than that of the bulk PEI and much lower than that of the "molecular basket" adsorbent with the same PEI loading, which also verified that only when the PEI was loaded into the channels of the mesoporous molecular sieve did the Si-MCM-41 exhibit the highest synergetic effect on the adsorption of CO_2. The CO_2 adsorption capacity of Silica Gel-PEI was nearly identical to that of the calculated CO_2 adsorption capacity on the external surface of the MCM-41 crystals. Satyapal et al. (2001) also

observed the same phenomenon when they coated the PEI on the high-surface-area solid polymethyl methacrylate polymeric support.

By employing the "molecular basket" concept, the CO_2 adsorption and desorption kinetics can also be improved significantly. Figure 3.4.15 compares the CO_2 adsorption curves of Si-MCM-41-PEI-50, Si-MCM-41-PEI-75 and PEI in the first minute (60 seconds) of adsorption. The CO_2 adsorption rate decreased in the following order: Si-MCM-41-PEI-50 > Si-MCM-41-PEI-75 > PEI. If the linear part of the adsorption curve was selected to calculate the CO_2 adsorption rate, the CO_2 adsorption rate was 5.60, 3.23, and 2.67 mg/s.g-PEI for Si-MCM-41-PEI-50, Si-MCM-41-PEI-75 and PEI, respectively. The CO_2 adsorption rate for Si-MCM-41-PEI-50 was much faster than that of the Si-MCM-41-PEI-75 and PEI, which confirmed that only when the PEI was loaded into the channels of the mesoporous molecular sieve did the Si-MCM-41 exhibit the highest synergetic effect and proved that the "molecular basket" concept resulted in the significant improvement in CO_2 adsorption by PEI. Coating PEI on the high surface area materials only slightly increased the CO_2 adsorption rate. The CO_2 desorption rate showed the same trend as the adsorption. The CO_2 desorption rate decrease in the following order: Si-MCM-41-PEI-50 > Si-MCM-41-PEI-75 > PEI. The CO_2 desorption was complete for Si-MCM-41-PEI-50 and Si-MCM-41-PEI-75 in 150 minutes, whereas only 56% of the adsorbed CO_2 was desorbed when the same desorption time as the Si-MCM-41-PEI adsorbent was used.

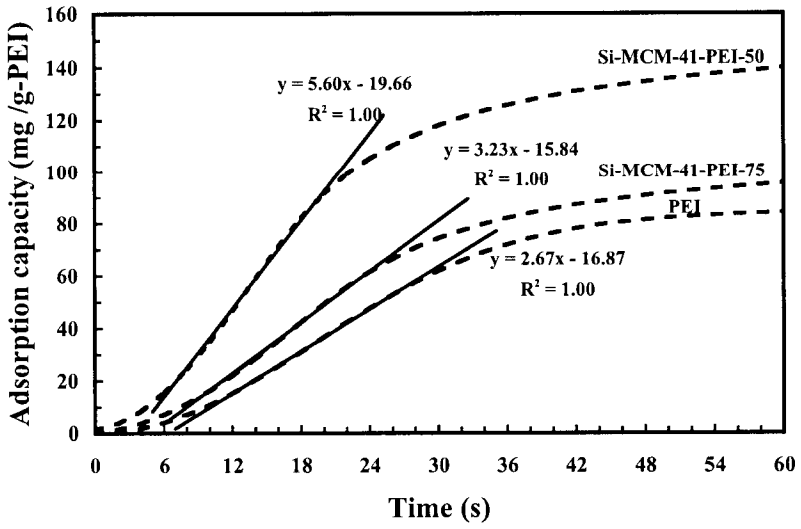

Figure 3.4.15 COMPARISON OF THE CO_2 ADSORPTION KINETICS OF Si-MCM-41-PEI-50, Si-MCM-41-PEI-75, AND PEI

When compared with conventional adsorbents, the "molecular basket" showed better CO_2 adsorption performance at relatively high temperature. Table 3.4.2 lists the CO_2 adsorption performance of zeolite, activated carbon, PEI/polymer composite and the "molecular basket" adsorbent. The "molecular basket" adsorbent showed superior CO_2 selectivity in terms of very high CO_2/N_2 ratios (>1,000 for MCM-41-PEI-50 vs 2-6 for aluminosilicates and activated carbons). The high selectivity for CO_2 is particularly important when it was applied in the separation of CO_2 from flue gas.

3.4.2.2 Adsorption Separation of CO_2 from Simulated Flue Gas

Adsorption Separation of CO_2 from Simulated Flue Gas

Figure 3.4.16 shows the breakthrough curve of CO_2 during the adsorption separation of the CO_2, N_2 and O_2 gas mixture by MCM-41-PEI-50. At the beginning of the separation, CO_2 was completely adsorbed by the adsorbent and the concentration of CO_2 was below the detection limit of the gas chromatography, i.e. < 100 ppm. After 50 minutes of adsorption, CO_2 began to break through and was detected in the effluent gas. The amount of break through concentration, C, was followed as a fraction of the CO_2 concentration in the feed gas mixture, C_0. At $\approx$ 55 minutes, the C/C_0 ratio was about 0.8, showing that the adsorbent still adsorbed 20% of the CO_2 in the feed. After 120 minutes of adsorption, the adsorbent can only adsorb 5% of the CO_2 from the feed.

In order to calculate the adsorption capacity, the volume of the adsorbed gases was calculated from the mass balance of the gas flow rate, the CO_2 concentration and the adsorption time. Figure 3.4.17 shows the normalized volume V_{ad}/V_0 (where V_{ad} equals to the volume of gases adsorbed and V_0 equals to the volume of gases feed into the system) of the adsorbed CO_2, N_2 and O_2 as a function of adsorption time. The CO_2 adsorption capacity was 45.4 ml (STP)/g adsorbent after 120 minutes. The adsorption capacity is comparable with that previously measured from the TGA as shown in Figure 3.4.18 at about 15% CO_2 concentration. If only the complete adsorption is considered, the adsorption capacity is 37.5 ml (STP)/g adsorbent. The adsorption of O_2 is much lower than that of the CO_2 and the adsorption capacity of O_2 is 0.07 ml (STP)/g adsorbent after 120 minutes. The separation factor for CO_2 and O_2 was calculated to be 185. The adsorbent hardly adsorbs any N_2. Therefore, the selective adsorption of CO_2 is

Table 3.4.2 Comparison of CO_2 Adsorption Performance of "Molecular Basket" Adsorbent and other Adsorbents

Adsorbents	Temp (°C)	Pressure (atm)	Adsorption Capacity (mg CO_2/g adsorbent)	CO_2/N_2 or CO_2/CH_4 selectivity	Reference
Si-MCM-41	25	1	27.3	--	this study
Si-MCM-41	75	1	8.6	--	this study
Si-MCM-41	75	0.149	6.3	2.9 (CO_2/N_2)	this study
Al-MCM-41-100	75	1	7.6	--	this study
Al-MCM-41-500	75	1	7.5	--	this study
Si-MCM-41-PEI-50	25	1	32.9	--	this study
Si-MCM-41-PEI-50	75	1	112	--	this study
Si-MCM-41-PEI-50	75	0.149	89.2	>1000 (CO_2/N_2)	this study
Al-MCM-41-100-PEI-50	75	1	127	--	this study
Al-MCM-41-500-PEI-50	75	1	121	--	this study
Zeolite 13 X	25	1	168	--	Siriwardane et al., 2001
Zeolite 4A	25	1	135	--	Siriwardane et al., 2001
Activated Carbon	25	1	110	--	Siriwardane et al., 2001
Norit RBI activated carbon	21.5	1	108	~ 2 (CO_2/CH_4)	Van der Vaart, et al., 2000
Norit RBI activated carbon	75	1	40	~ 2 (CO_2/CH_4)	Van der Vaart, et al., 2000
Activated carbon	20	1	88	~ 2 (CO_2/CH_4)	Berlier aand Frere, 1997
Norit RBI activated carbon	25	1	140.8	~ 1.9 (CO_2/CH_4)	Dreisbach, et al, 1999
PEI-silica gel	75	1	78.1	--	this study
PEI-polymer	~ 50	0.02	~ 40	--	Kohl and Nielsen, 1997

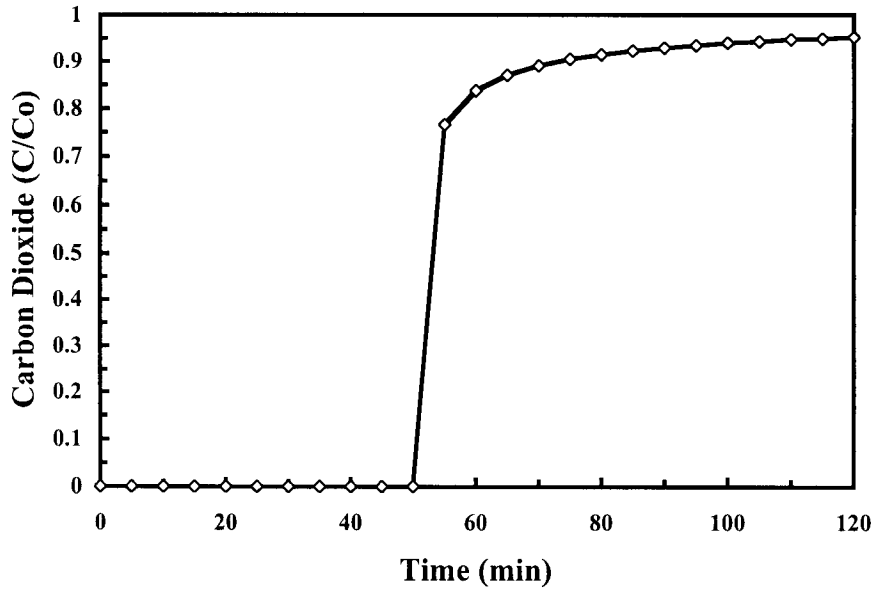

Figure 3.4.16 BREAKTHROUGH CURVE OF CO_2 WITH MCM-41-PEI-50 (Operating conditions: weight of adsorbent: 2.0 g; feed composition: 14.9% CO_2, 4.25% O_2 and 80.85% N_2; feed flow rate: 10 ml/min; temperature: 75°C)

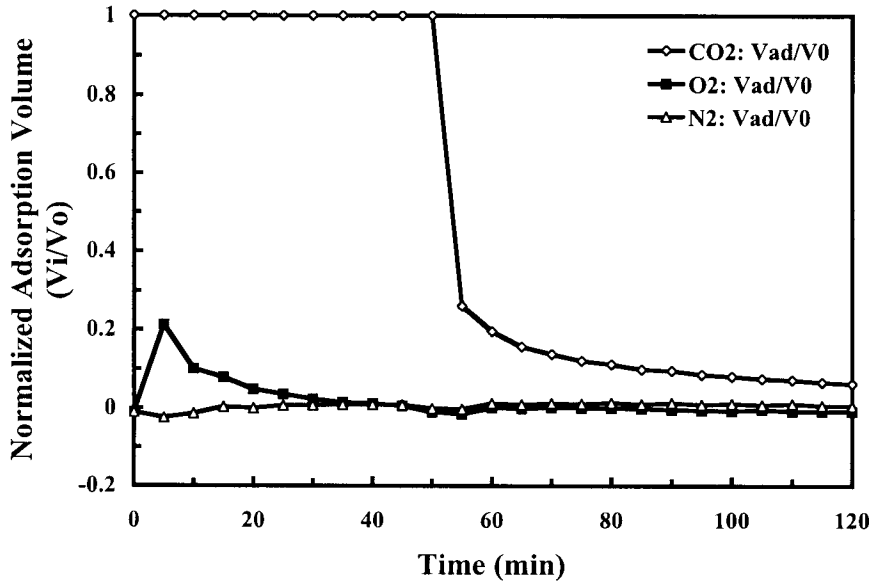

Figure 3.4.17 NORMALIZED ADSORPTION VOLUME OF CO_2, O_2 AND N_2 (V_{ad}/V_0) AS A FUNCTION OF ADSORPTION TIME DURING THE ADSORPTION SEPARATION OF CO_2 FROM SIMULATED FLUE GAS MIXTURE BY "MOLECULAR BASKET" ADSORBENT (V_{ad}: volume of CO_2, O_2 or N_2 adsorbed; V_0: volume of CO_2, O_2 or N_2 feed into the system)

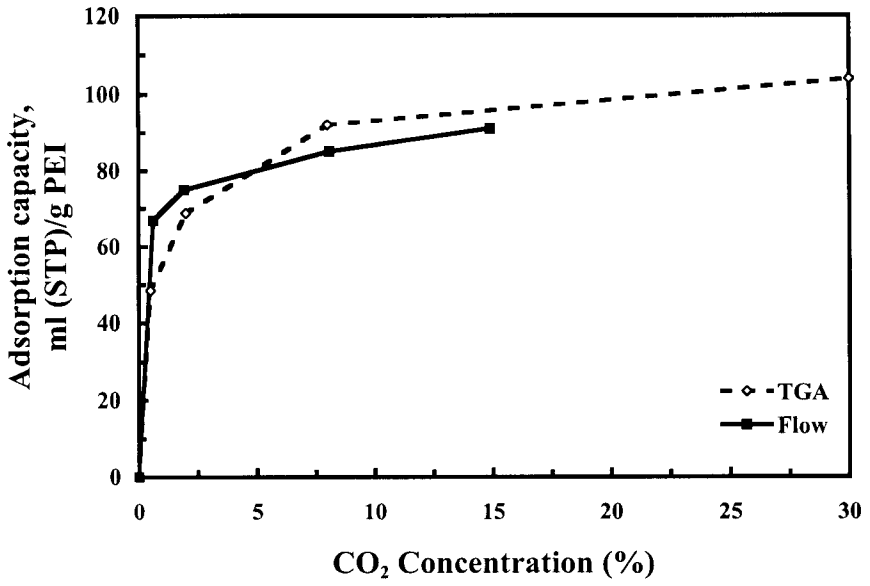

Figure 3.4.18 THE ADSORPTION CAPACITY OF MCM-41-PEI-50 AS A FUNCTION OF FEED CO_2 CONCENTRATION MEASURED BY BOTH TGA AND THE FLOW ADSORPTION SYSTEM

realized by loading the PEI into the MCM-41 channels. For molecular sieves or zeolites from other studies, the separation factor of CO_2 over other gases was only around 2.

The Influence of Operating Conditions on the Separation of CO_2 from Simulated Flue Gas Mixtures

The Influence of Temperature on the Adsorption Separation of CO_2

The influence of operating temperature on the adsorption separation of CO_2, N_2 and O_2 gas mixture was investigated. Figure 3.4.19 shows the breakthrough curve of CO_2 at different temperatures. The higher the operating temperature, the more CO_2 was adsorbed. The adsorption capacities were 19.3, 28.8, 45.4, and 47.4 ml (STP)/g adsorbent for 25, 50, 75, and 100°C, respectively. The desorption of CO_2 at low temperature was very slow and not complete, which is in accordance with the results by TGA. The desorption capacity was only ≈10 and 15% at 25 and 50°C, respectively. The desorption was complete at 75°C.

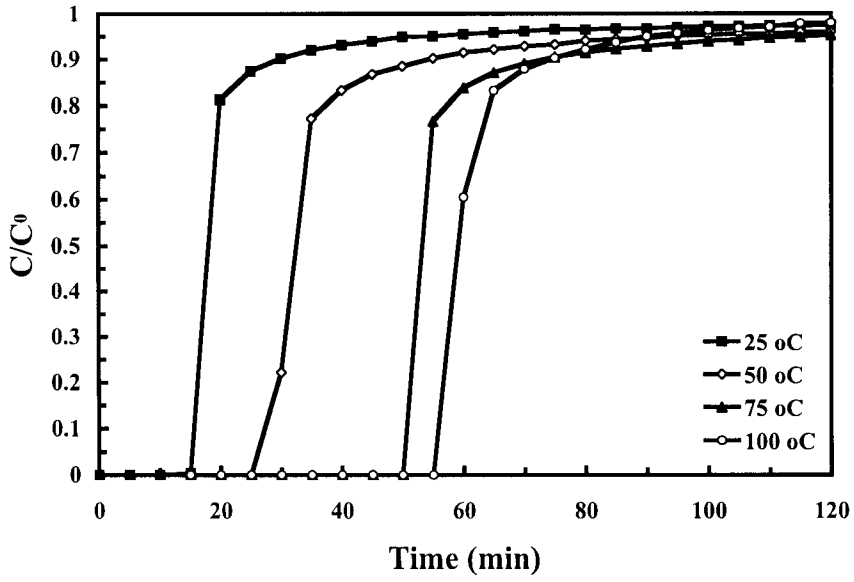

Figure 3.3.19 THE INFLUENCE OF OPERATING TEMPERATURE ON THE BREAKTHROUGH CURVE OF CO_2 (Operating conditions: weight of adsorbent: 2.0 g; feed composition: 14.9% CO_2, 4.25% O_2 and 80.85% N_2; feed flow rate: 10 ml/min)

The Influence of Feed Flow Rate on the Adsorption Separation of CO_2

The influence of the feed flow rate on the adsorption capacity was investigated and the results are shown in Figure 3.4.20. The total adsorption capacities at 120 minutes were nearly identical among the three flow rates investigated. However, the adsorption capacity for the zero carbon dioxide emissions was different. The lower the feed flow rate, the higher the adsorption capacity for the zero CO_2 emissions. The adsorption capacities for the zero CO_2 emissions were 75, 74, and 67 ml (STP)/g adsorbent for the feed flow rate of 10, 20, and 30 ml/min, respectively.

The Influence of CO_2 Concentration in the Feed on the Adsorption Separation of CO_2

Since the CO_2 concentration in flue gas varies depending on the combustion processes and conditions used, the influence of CO_2 concentration in the feed on the adsorption performance was investigated. The CO_2 breakthrough curves are shown in Figure 3.4.21. The lower the CO_2 concentration was in the gas mixture, the longer the time it took to achieve zero CO_2 emissions. However, the total adsorption capacities increased with increasing CO_2 concentration and were 33.3, 35.5, 42.5, and 45.5 ml (STP)/g adsorbent for carbon dioxide concentrations of 0.652, 1.94, 8.09, and 14.9%, respectively. The adsorption capacities are

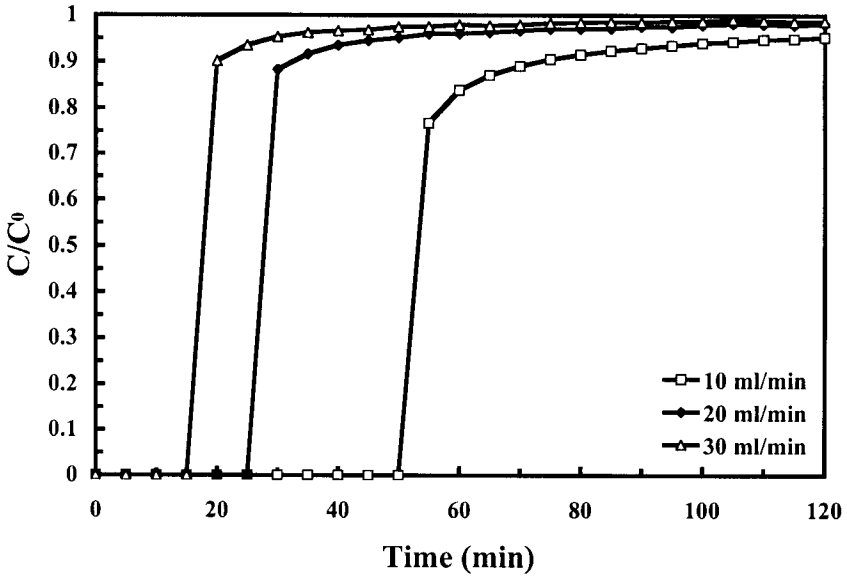

Figure 3.4.20 THE INFLUENCE OF FEED FLOWRATE ON THE BREAKTHROUGH CURVE OF CO_2 (Operating conditions: weight of adsorbent: 2.0 g; feed composition: 14.9% CO_2, 4.25% O_2 and 80.85% N_2; temperature: 75°C)

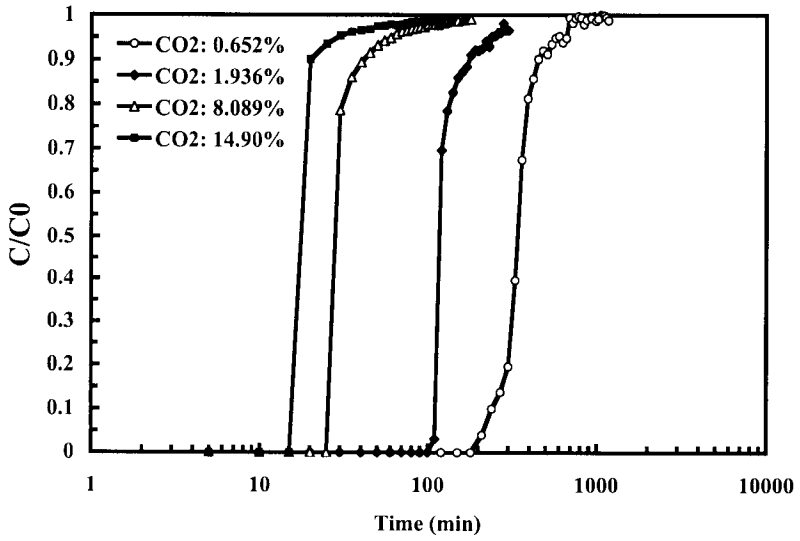

Figure 3.4.21 THE INFLUENCE OF FEED CO_2 CONCENTRATION ON THE BREAKTHROUGH CURVE OF CO_2 (Operating conditions: weight of adsorbent: 2.0 g; temperature: 75°C; feed flow rate: 30 ml/min)

compared with those previously obtained from TGA in Figure 3.4.18. At low CO_2 concentrations, the adsorption capacities from the flow system were somehow higher than those from the TGA measurements. The higher adsorption capacities for the flow system may be caused by the longer adsorption time of 20 h used for the flow system as compared to 2.5 h for the TGA. When the adsorption time for the flow system was shortened from 20 h to 6 h for the feed with a CO_2 concentration of 0.652%, the adsorption capacity decreased from 33.3 to 28.9 ml (STP)/g. The adsorption capacity was close to that of 25.5 ml (STP)/g adsorbent obtained by the TGA measurement. With increasing CO_2 concentration in the feed, the adsorption capacity in the flow system is lower than that from the TGA measurement. The slightly reduced adsorption capacity may be caused by the inhomogeneous temperature distribution along the adsorbent bed. The temperature in this experiment was only measured in the center part of the adsorbent bed. At the beginning or end of the adsorbent bed, the temperature could be 8°C lower than at center bed, which will result in a lower adsorption capacity.

The Influence of Moisture on the Adsorption Separation of CO_2

Since the flue gas contains about 8-20% moisture, the influence of moisture on the adsorption of CO_2 was investigated. Figure 3.4.22 compares the breakthrough curve of CO_2 for the feed gas without moisture and with 10% moisture. The adsorption of CO_2 increases when moisture is added to the feed. The adsorption capacity was increased from 47.4 ml (STP)/g adsorbent for dry feed to 63.7 ml (STP)/g adsorbent for moist feed. At the same time, the water was also adsorbed into the adsorbent. The adsorption capacity of water was 58.5 ml (STP)/g adsorbent.

The increase in the CO_2 capacity can be ascribed to reactions (3.4.1) and (3.4.2) for the dry condition, and to reactions (3.4.3), (3.4.4), and (3.4.5) for the moist condition:

$$CO_2 + 2RNH_2 \Leftrightarrow NH_4^+ + R_2NCOO^- \qquad (3.4.1)$$

$$CO_2 + 2R_2NH \Leftrightarrow R_2NH_2^+ + R_2NCOO^- \qquad (3.4.2)$$

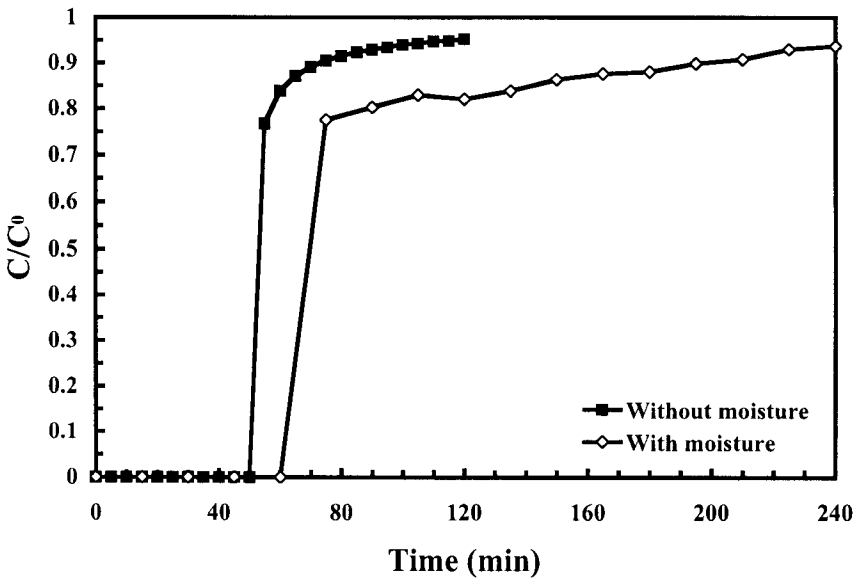

Figure 3.4.22 COMPARISON OF THE CO_2 BREAKTHROUGH CURVE IN THE ABSENCE AND IN THE PRESENCE OF 10% MOISTURE (Operating conditions: weight of adsorbent: 2.0 g; temperature: 75°C; feed flow rate: 10 ml/min)

Reactions (3.4.1) and (3.4.2) show that 2 moles of amine are needed under dry conditions to adsorb one mole of carbon dioxide. When moisture was added to the feed, the carbamate ion formed in reactions (3.4.1) and (3.4.2) will further react with CO_2 and H_2O to form bicarbonate (reaction (3.4.3)). The amine itself can also react directly with CO_2 and H_2O (reaction (3.4.4) and (3.4.5)).

$$R_2NCOO^- + 2H_2O + CO_2 \Leftrightarrow R_2NH_2^+ + 2HCO_3^- \quad (3.4.3)$$

$$CO_2 + RNH_2 + H_2O \Leftrightarrow RNH_3^+ + HCO_3^- \quad (3.4.4)$$

$$CO_2 + R_2NH + H_2O \Leftrightarrow R_2NH_2^+ + HCO_3^- \quad (3.4.5)$$

Therefore, in the presence of water, one mole of amine can adsorb one mole of carbon dioxide.

The effect of moisture on the enhancement of the adsorption capacity can further be verified by changing the moisture concentration in the feed. Table 3.4.3 shows the relationship between the adsorption capacity and the moisture concentration in the feed. At low moisture concentration, the adsorption capacity increased rapidly with increasing moisture concentration

in the feed. However, when the moisture concentration reached 16%, the increase in the adsorption capacity slowed. It is also noteworthy that the adsorption capacities increased even though the CO_2 concentration in the feed decreased. This is opposite of that observed for the dry condition. According to reactions (3.4.4) and (3.4.5), the formation of bicarbonate needs one mole of H_2O per mole of CO_2. When the moisture concentration is lower than that of the CO_2, the adsorption capacity of CO_2 increases rapidly with increase in moisture concentration. When the moisture concentration is larger than that of the CO_2, the CO_2 adsorption capacity can not be further increased by the excess water. The above phenomena indicated strongly that the presence of water has a synergetic effect on the CO_2 adsorption capacity.

Table 3.4.3 The Influence of Moisture Concentration on the Adsorption Separation of Carbon Dioxide from the Simulated Flue Gas

Feed concentration (%)				CO_2 adsorption capacity (ml (STP)/g adsorbent)
CO_2	N_2	O_2	H_2O	
14.90	80.85	4.25	---	45.5
13.91	75.71	3.95	6.43	54.0
13.55	72.72	3.86	9.87	63.7
12.61	68.25	3.56	15.59	66.8

The Influence of Sweep Gas Flow Rate on Desorption of CO_2

Three helium sweep gas flow rates of 10, 20, and 50 ml/min were selected to clarify the effect of the sweep gas flow rate on the desorption of carbon dioxide after an adsorption experiment. The results are shown in Figure 3.4.23. With increasing sweep gas flow rate, the desorption rate of the carbon dioxide increases. Desorption at 300 minutes was not complete when the sweep gas flow rates were 10 and 20 ml/min and the desorption capacities were 48 and 76%, respectively. When the sweep gas flow rate was increased to 50 ml/min, desorption was complete after 300 minutes. This indicated that the regeneration of the adsorbent can easily be optimized.

Stability of the "Molecular Basket" Adsorbent

Thermal Stability of the "Molecular Basket" Adsorbent

The stability of the adsorbent was investigated at 75 and 100°C. The successive adsorption and desorption cycles were carried out at 75 and 100°C, and the results are shown in

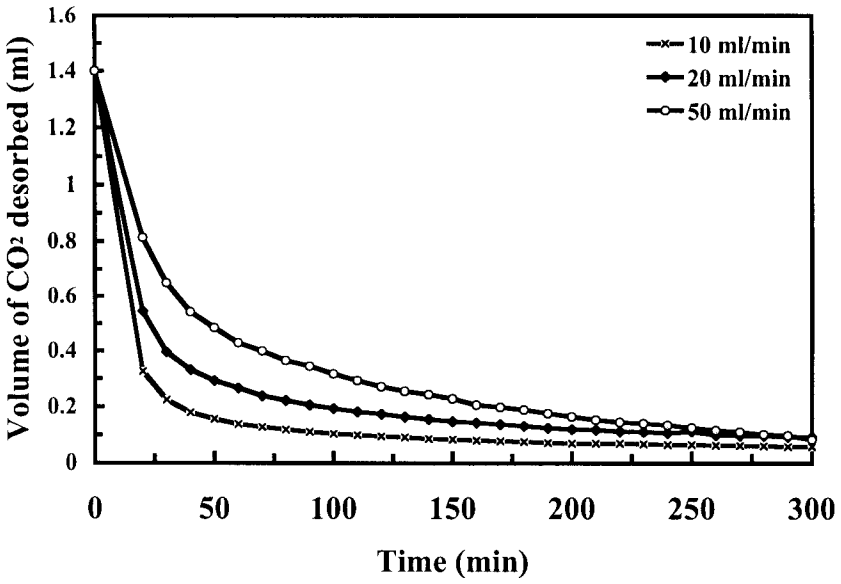

Figure 3.4.23 THE INFLUENCE OF SWEEP GAS FLOW RATE ON THE DESORPTION OF CO_2 (Operating conditions: weight of adsorbent: 2.0 g; temperature: 75°C; feed flow rate: 10 ml/min)

Figures 3.4.24 and 3.4.25, respectively. At 75°C, the adsorption capacity did not change between the successive measurements, indicating that the adsorption performance was stable. However, when the operating temperature was increased to 100°C, there was a decrease in the adsorption capacity in the second measurement. The adsorption capacity in the second measurement was 43.6 ml (STP)/g adsorbent, and was about 8% lower than that of the first measurement of 47.4 ml (STP)/g adsorbent. The deactivation of the adsorbent is caused by oxidation of the polymer at this relatively high temperature. Figure 3.4.26 shows that there is a significant increase in the O_2 consumption at 100°C, when compared to that at 75°C. The consumption of O_2 increases from 0.12 ml (STP)/g adsorbent at 75°C to 5.1 ml (STP)/g adsorbent at 100°C. Further, the amount of O_2 desorbed after the adsorption at 100°C is only 0.06 ml (STP)/g adsorbent, which represents only 1% of the consumed oxygen. In addition, the color of the adsorbent turned from white in its original form to pale yellow after the adsorption measurement at 100°C. Therefore, the increased consumption of O_2 with increasing temperature has been linked to the oxidation of the polymer, indicating that the adsorbent is not suitable for use at temperatures higher than 100°C.

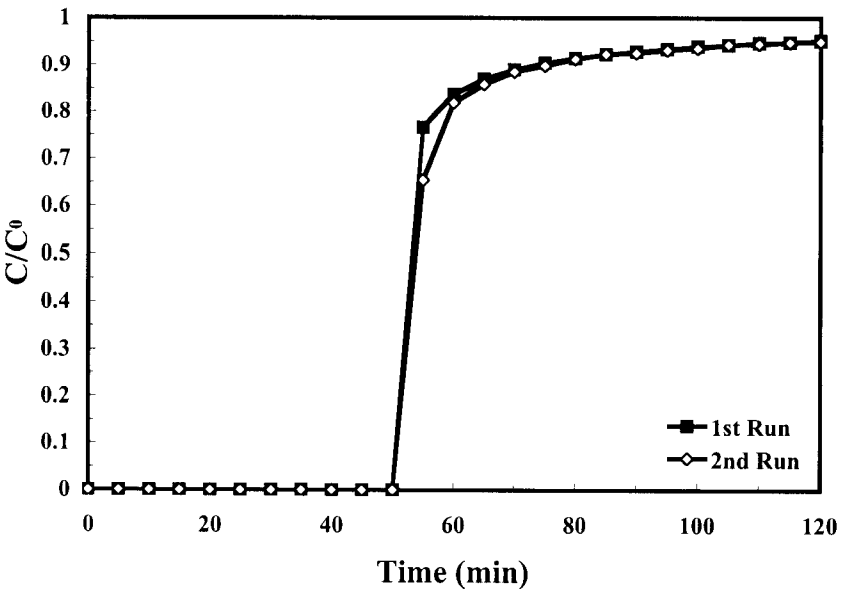

Figure 3.4.24 STABILITY OF THE ADSORBENT AT 75°C. (Operating conditions: weight of adsorbent: 2.0 g; temperature: 75°C; feed flow rate: 10 ml/min)

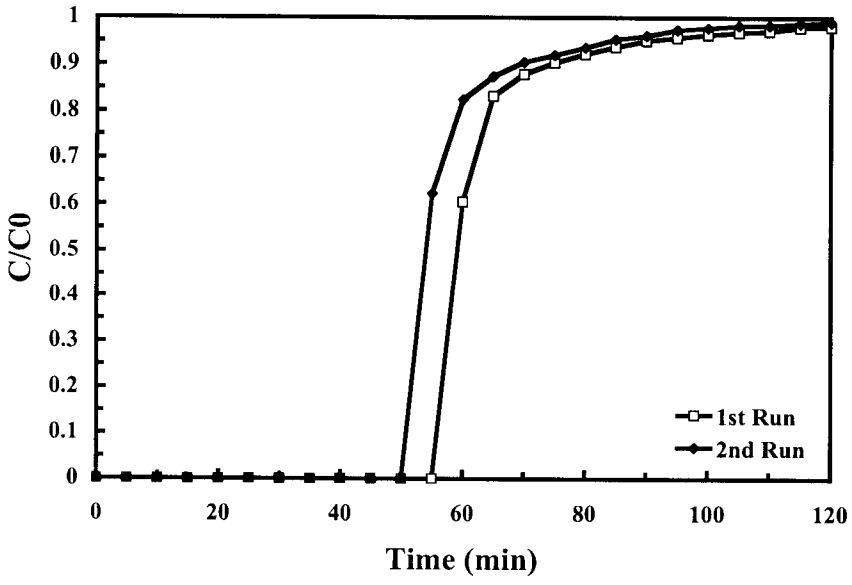

Figure 3.4.25 STABILITY OF THE ADSORBENT AT 100°C. (Operating condition: weight of adsorbent: 2.0 g; temperature: 100°C; feed flow rate: 10 ml/min)

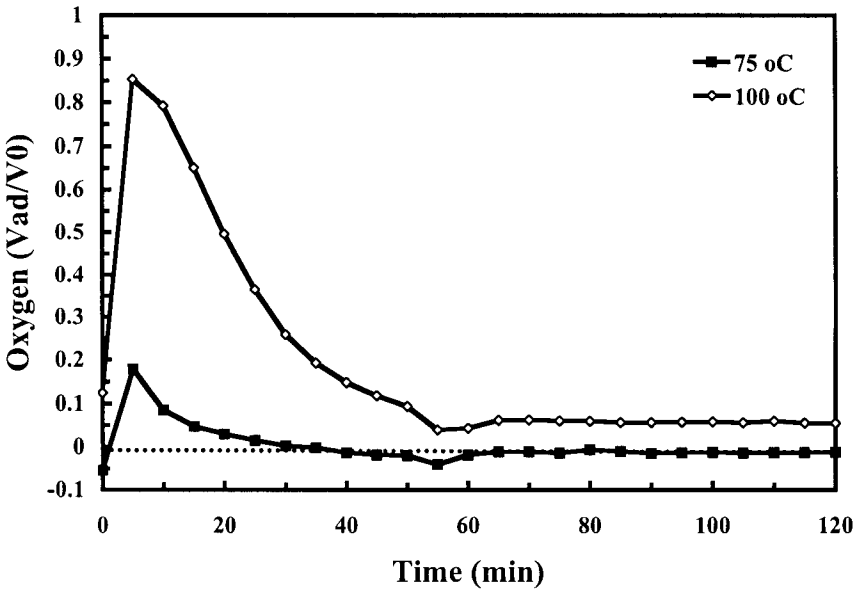

Figure 3.4.26 COMPARISON OF THE OXYGEN "ADSORPTION" AT DIFFERENT TEMPERATURES INDICATING THE DEGREE OF OXIDATION OF THE POLYMER (Operating conditions: weight of adsorbent: 2.0 g; feed flow rate: 10 ml/min)

Cyclic Adsorption/Desorption Stability

Cyclic Adsorption/Desorption Stability Under Dry Flue Gas Conditions. For practical applications, the adsorbent should not only possess high selectivity and high adsorption capacity, but must also exhibit stable adsorption and desorption performance for thousands of cycles. In this study, cyclical adsorption and desorption were carried out, and the results are shown in Figure 3.4.27. During ten cycles of operation, the CO_2 adsorption capacity was relatively unchanged, indicating the adsorbent is stable in the separation process. Desorption was also complete. The adsorption selectivity also did not change in the ten cycles of operation. The stable adsorption and desorption performance suggests that this adsorbent is promising for practical applications.

Stable adsorption and desorption performance is a key issue for a adsorbent using a chemical adsorption mechanism. Bakker et al. (1973) observed that CO_2 adsorption capacity decreased 40% for a CaO adsorbent after five cycles of operation at 866°C. The author suggested that the decrease in adsorption capacity was due to the formation of a nonporous $CaCO_3$ layer on the particle surface. This layer hindered the inward diffusion of CO_2. Cyclical experiments conducted at a carbonation temperature of 880°C and a calcination temperature of

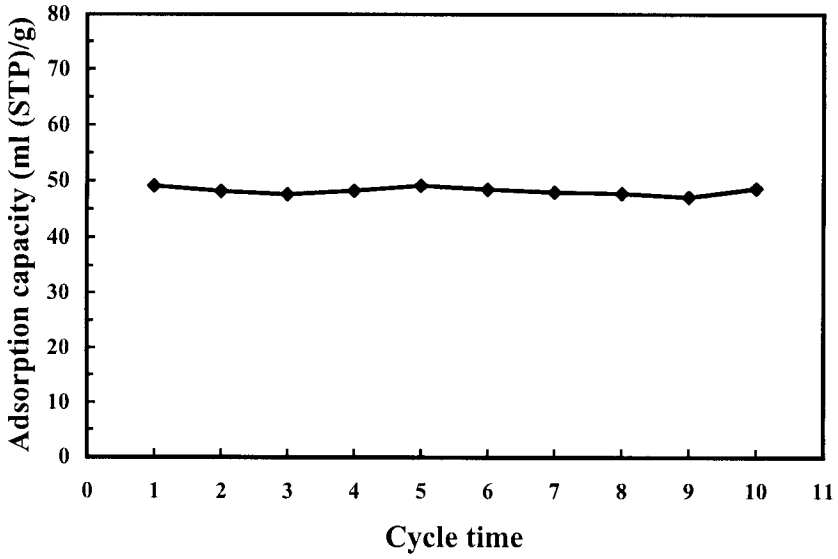

Figure 3.4.27 STABILITY OF THE "MOLECULAR BASKET" ADSORBENT UNDER DRY FLUE GAS CONDITIONS (Operating conditions: weight of adsorbent: 2.0 g; feed composition: 14.9% CO_2, 4.25% O_2 and 80.85%; temperature: 75°C; Feed flow rate: 10 ml/min)

860°C led to a drop in conversion of CaO to $CaCO_3$ from 70% in the first carbonation to 38% in the 7th carbonation step. The "molecular basket" adsorbent was stable after ten cycles of operation. Since the active species of PEI was uniformly dispersed into the mesoporous molecular sieve of MCM-41with a uniform pore size of around 3 nm, the diffusion of CO_2 to the active site was not hindered. Using the same reasoning, the adsorbent was easily regenerated. However, when bulk PEI was used as the adsorbent, a diffusion hindrance was observed (Xu et al., 2002b). The bulk PEI showed not only a low adsorption capacity, but also an incomplete desorption. The "molecular basket" adsorbent was also stable at relatively high temperature, e.g., 75°C. In addition, the structure of MCM-41 was well preserved after ten cycles of separation as evidenced in Figure 3.4.28 for the XRD characterization results before and after the adsorption separation. The stable structure of MCM-41 is of critical importance to the "molecular basket" effect of the adsorbent (Xu, et al., 2002a,b; Xu et al., 2003).

Cyclic Adsorption/Desorption Stability under Moist Flue Gas Conditions. In practical situations, water vapor is often contained in the gas mixture, e.g., ≈10% water vapor in flue gas. Adsorption separation under such high moisture conditions is not well characterized. In addition, zeolite and molecular sieves are not stable in moist atmospheres at high temperature.

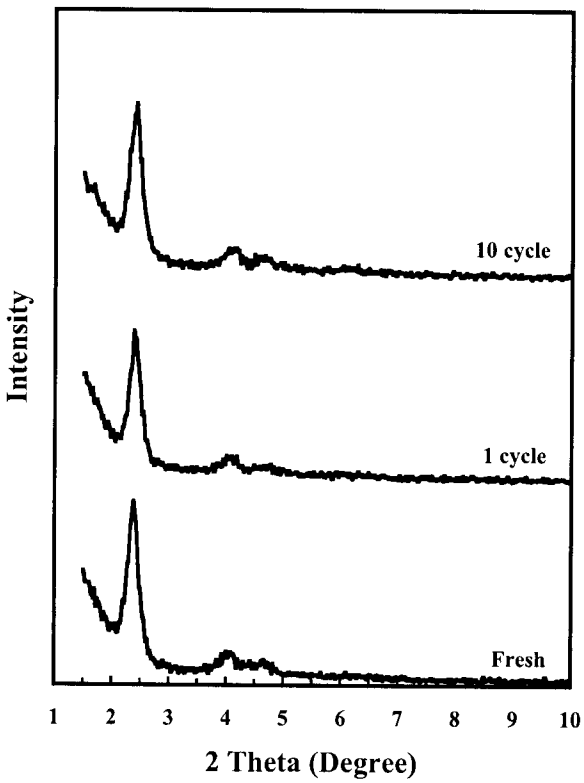

Figure 3.4.28 XRD PATTERNS OF THE "MOLECULAR BASKET" ADSORBENT BEFORE AND AFTER CYCLIC OPERATION UNDER DRY FLUE GAS CONDITIONS AT 75°C

In this study, cyclical adsorption and desorption were carried out under moist conditions, and the results are shown in Figure 3.4.29. During ten cycles of operation, the CO_2 adsorption capacity remained relatively unchanged, indicating the adsorbent was stable in the separation process. The CO_2 adsorption capacity varied between 69.0 to 72.4 ml (STP)/g adsorbent. Note that the CO_2 and H_2O concentration also varied slightly in the feed during the ten cycles of operation. Desorption was also complete. The adsorption selectivity also did not change in the ten cycles of operation.

The structure of MCM-41 and MCM-41-PEI before and after adsorption separation was characterized by XRD. Figure 3.4.30 shows the XRD patterns of MCM-41 and Figure 3.4.31 shows the XRD patterns of the "molecular basket" adsorbent. The structure of MCM-41 collapsed only after 1 cycle operation under the 10% moisture condition. However, the structure of MCM-41 was preserved even after 10 cycles of operation, which indicated that loading PEI into the channels of MCM-41 protected the structure of MCM-41. It is well known that MCM-

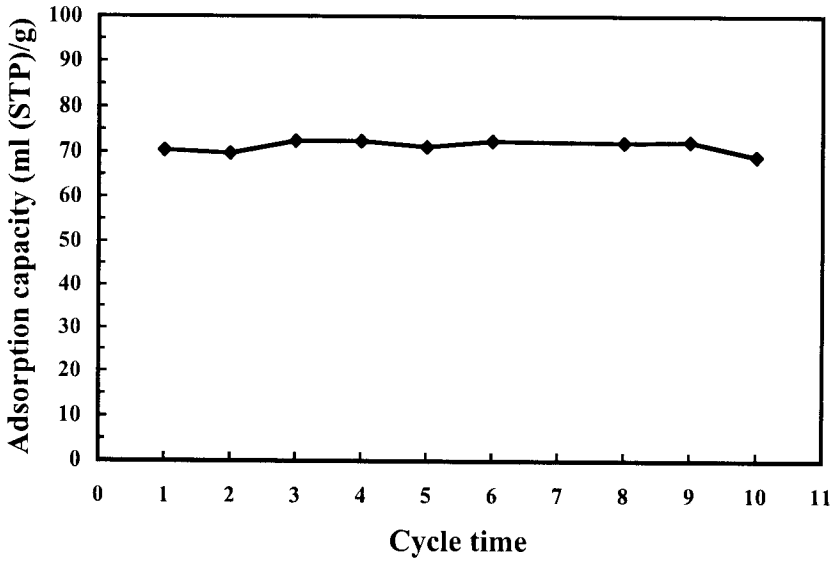

Figure 3.4.29 STABILITY OF THE "MOLECULAR BASKET" ADSORBENT UNDER MOIST FLUE GAS CONDITIONS (Operating conditions: weight of adsorbent: 2.0 g; feed composition: 13.4 % CO_2, 3.8% O_2, 10.4% H_2O and 72.4 %; temperature: 75°C; feed flow rate: 10 ml/min)

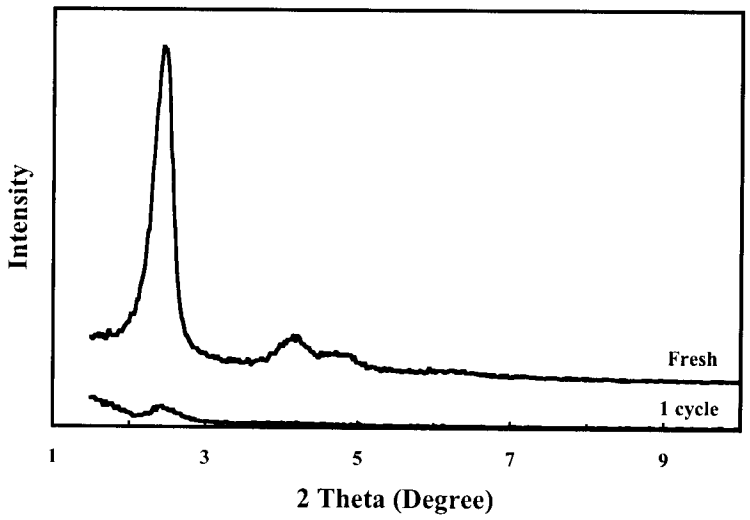

Figure 3.4.30 XRD PATTERNS OF MCM-41 BEFORE AND AFTER OPERATING UNDER MOIST SIMULATED FLUE GAS CONDITIONS AT 75°C

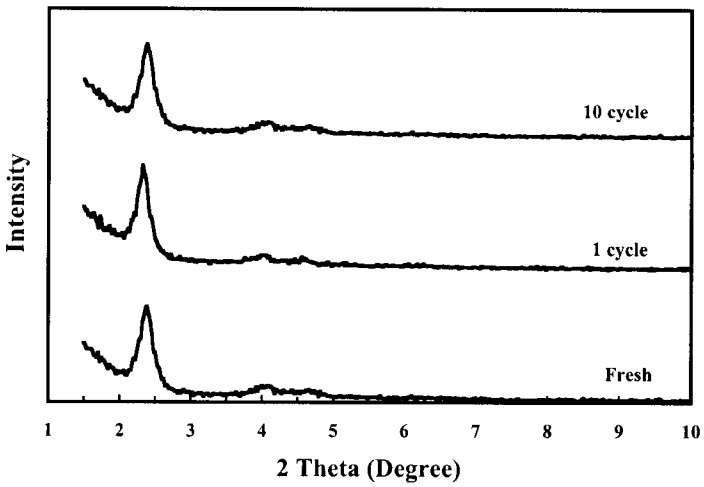

Figure 3.4.31 XRD PATTERNS OF THE "MOLECULAR BASKET" ADSORBENT BEFORE AND AFTER OPERATING UNDER MOIST SIMULATED FLUE GAS CONDITIONS AT 75°C.

41 is unstable in the presence of moisture, even at medium temperatures. The collapse of the MCM-41 structure was caused by the reaction between MCM-41 and water. Since the PEI is more hydrophilic than MCM-41, the adsorption of water by PEI is stronger than for the MCM-41. Therefore, the structure of MCM-41 was protected after the PEI was loaded into the MCM-41. Preservation of the MCM-41 structure is critically important for the adsorption separation performance of this novel "molecular basket" adsorbent.

3.4.2.3 Adsorption Separation of Boiler Flue Gas

Adsorption Separation of Natural Gas-Fired Flue Gas

Typical CO_2 breakthrough curves for the 'molecular basket" adsorbent and the blank "alumina" are shown in Figure 3.4.32 for the natural gas-fired flue gas. Clearly, both the alumina and the "molecular basket" adsorbent adsorbed CO_2. However, the adsorption performance of the "molecular basket" adsorbent was much better than that of the alumina. The lowest CO_2 emission concentration was $\approx$ 0.8% for alumina, while it was less than 0.1% for the "molecular basket" adsorbent. The CO_2 adsorption capacity was 26 ml (STP)/g adsorbent for the "molecular basket" adsorbent and 1.1 ml (STP)/g adsorbent for the alumina. In addition, the "molecular basket" adsorbent showed better selectivity. The "molecular basket" adsorbent did not adsorb O_2, N_2 and CO while the CO_2/O_2 selectivity was 3.5 for alumina. The adsorption

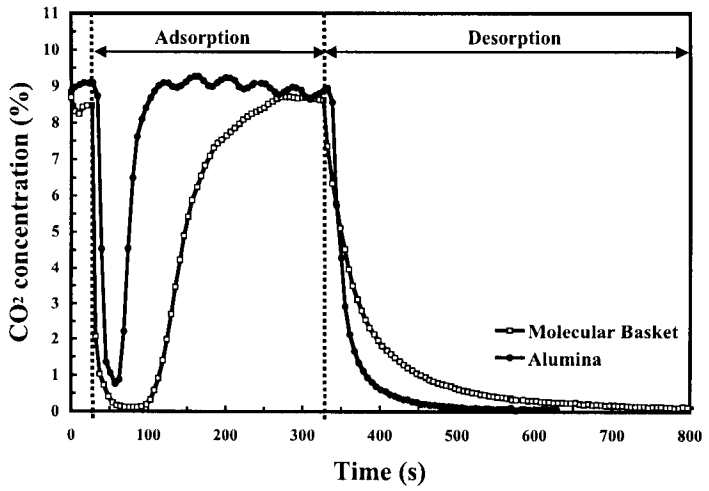

Figure 3.4.32 BREAKTHROUGH CURVE OF CO_2 FOR FLUE GAS FROM NATURAL GAS-FIRED BOILER

capacity of NO_x for the "moleculae basket" adsorbent was higher than that for alumina, as shown in Figure 3.4.33. The NO_x adsorption capacity was 0.0505 ml (STP)/g adsorbent for the "molecular basket" adsorbent and $7.5*10^{-4}$ ml (STP)/g adsorbent for the alumina. The selectivity of CO_2/NO_x was 0.45 for the "molecular basket" adsorbent. However, very little NO_x was absorbed before CO_2 breakthrough. The CO_2 and NO_x adsorption capacities before CO_2 breakthrough were 21 ml (STP)/g adsorbent and $7.1*10^{-3}$ ml (STP)/g adsorbent, respectively. Therefore, the selectivity of CO_2/NO_x was 2.5. Further, while the desorption of CO_2 was complete, very little NO_x desorbed.

Adsorption Separation of Coal-Fired Flue Gas

The adsorption separation of CO_2 from coal-fired flue gas was also investigated. In the coal fired flue gas, there was a significant concentration of SO_2. The adsorption separation results are shown in Figures 3.4.34 to 3.4.36. Similar trends were observed for the coal-fired flue gas as for the natural gas-fired flue gas. The adsorptions of N_2 and O_2 by the "molecular basket" adsorbent were below the detect limit of the apparatus. The adsorption capacities for CO_2, SO_2 and NO_x were 36, 0.11, and 0.21 ml (STP)/g adsorbent, respectively. The separation selectivities for CO_2/SO_2 and CO_2/NO_x were 1.07 and 0.57, respectively. The adsorption capacities for CO_2, SO_2 and NO_x before CO_2 breakthrough were 24, 0.0074, and 0.028 ml (STP)/g adsorbent, respectively. Therefore, the separation selectivities for CO_2/SO_2 and

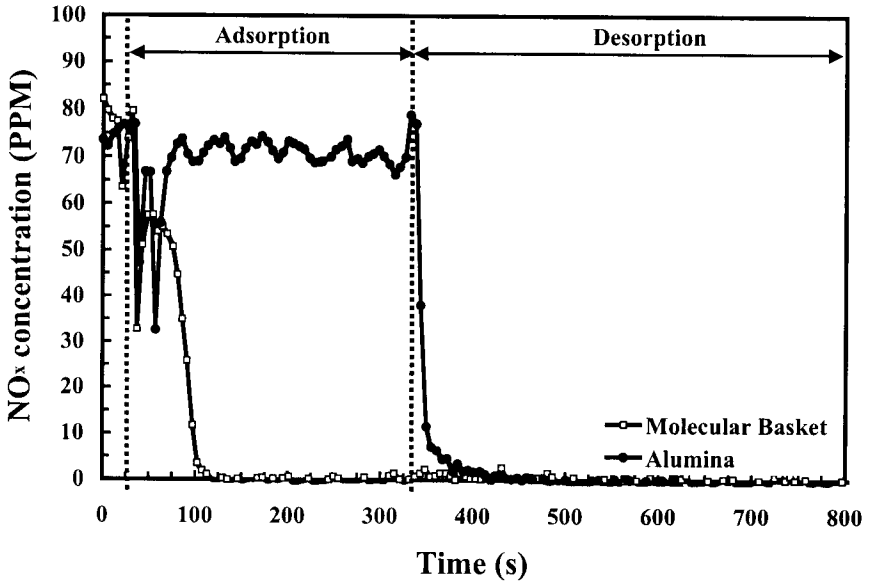

Figure 3.4.33 NO_x CONCENTRATION CHANGE DURING THE SEPARATION OF FLUE GAS FROM A NATURAL GAS-FIRED BOILER

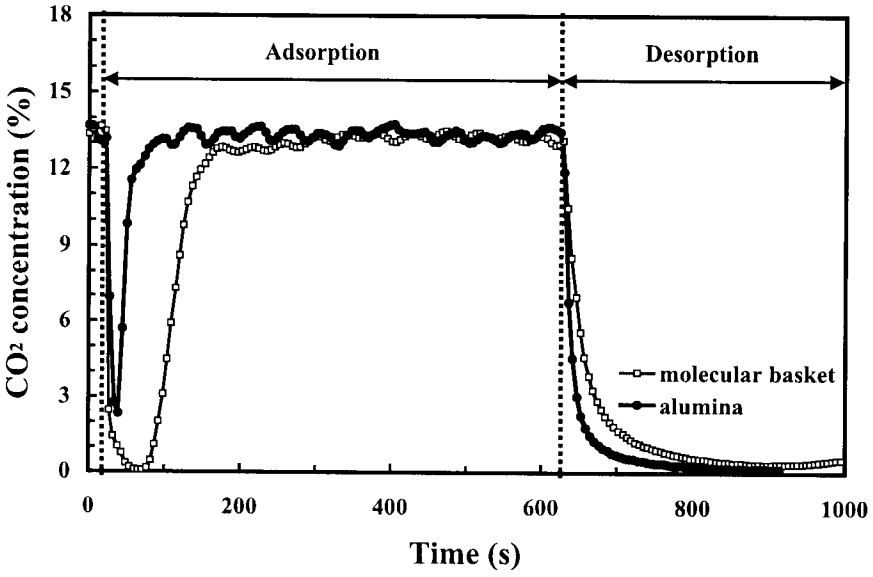

Figure 3.4.34 BREAKTHROUGH CURVE OF CO_2 FOR FLUE GAS FROM A COAL-FIRED BOILER

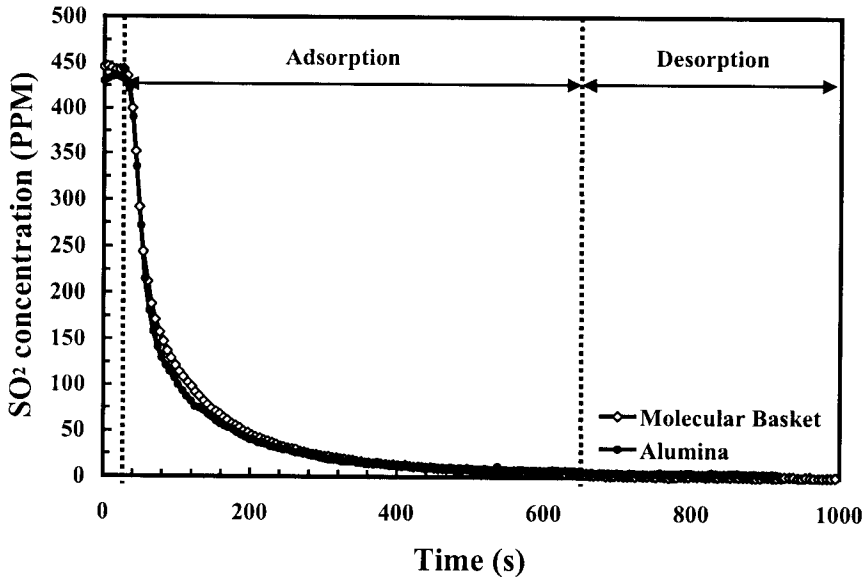

Figure 3.4.35 SO_2 CONCENTRATION CHANGE DURING THE SEPARATION OF A COAL-FIRED FLUE GAS MIXTURE

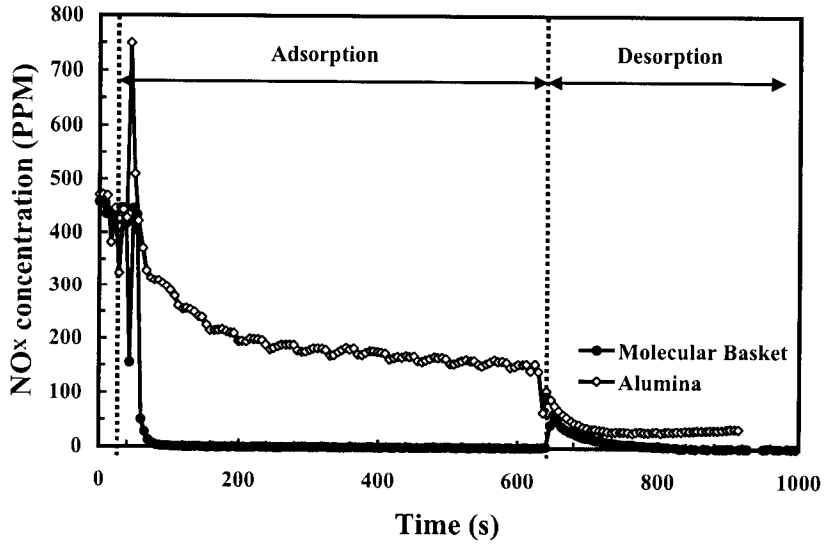

Figure 3.4.36 NO_x CONCENTRATION CHANGE DURING THE SEPARATION OF A COAL-FIRED FLUE GAS MIXTURE

CO_2/NO_x were 10.7 and 2.86, respectively, before CO_2 breakthrough. Again, while desorption of CO_2 was complete, very little NO_x and SO_2 desorbed.

Compared with the adsorption capacity in the simulated flue gas, the adsorption capacity in the boiler flue gas was about 30% lower at similar feed compositions. The adsorption capacity for the coal-fired flue gas was 36 ml (STP)/g adsorbent at 80±10°C for the feed composition of 12.5-12.8% CO_2, ≈4.4% O_2, 50 ppm CO, 420 ppm NO_x, 420 ppm SO_2, 6.2% H_2O and 76-77% N_2. The adsorption capacity for the simulated flue gas mixture was 53 ml (STP)/g adsorbent at 75°C for the feed composition of 13.9% CO_2, 3.95% O_2, 6.43% H_2O and 75.7% N_2. There are several explanations for the difference in adsorption capacity. First, the CO_2 concentration in the coal-fired flue gas mixture was lower than that in the simulated flue gas mixture. At low CO_2, concentration, the CO_2 adsorption capacity will be low. Second, different physical forms of the adsorbent will have different CO_2 adsorption capacities. A comparison study on the CO_2 adsorption of a powder adsorbent and a pellet adsorbent was carried out and the results are shown in Figure 3.4.37. It is evident in Figure 3.4.37 that the pellet adsorbent had

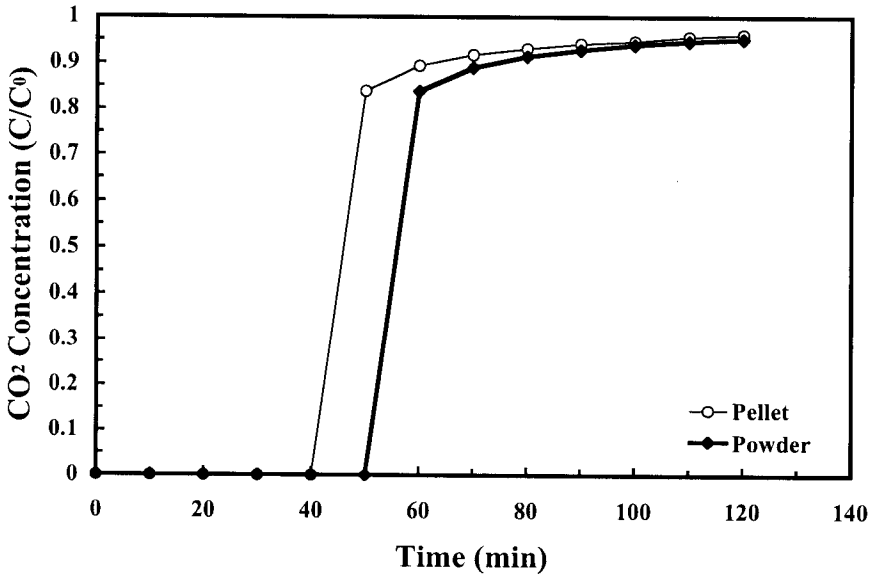

Figure 3.4.37 COMPARISON OF THE CO_2 BREAKTHROUGH CURVE OF THE "MOLECULAR BASKET" ADSORBENT IN PELLET AND IN POWDER FORM (Operating conditions: weight of adsorbent: 2.0 g; feed composition: 14.9% CO_2, 4.25% O_2 and 80.85%; temperature: 75°C; feed flow rate: 10 ml/min)

a lower adsorption capacity than the power adsorbent. The adsorption capacity of the pellet adsorbent was 42 ml (STP)/g adsorbent and was 10% lower than that of the powder adsorbent. Third, the higher flow rate in the boiler flue gas separation contributed to the lower adsorption capacity. The feed flow rate was 167 ml/min/g adsorbent in the boiler flue gas separation and was 5 ml/min/g adsorbent in the simulated flue gas separation. Lastly, the minor gas components, i.e., NO_x and SO_2, influenced the adsorption of CO_2. Since NO_x and SO_2 are acid gases and the adsorbent is basic in nature, the NO_x and SO_2 are competitive adsorbates for CO_2. These experimental results showed that adsorption of NO_x by the "'molecular basket" adsorbent was even stronger than that of CO_2 under some experimental conditions. The pre-removal of NO_x and SO_2 from the flue gas mixture is therefore required for the adsorption separation of CO_2 from the flue gas mixture by this "molecular basket" adsorbent.

3.4.3 Conclusions

Novel CO_2 "molecular basket" adsorbents based on a polyethylenimine (PEI)-modified mesoporous molecular sieve of MCM-41 type (MCM-41-PEI) were successfully developed. The highest CO_2 adsorption capacity obtained was 246 mg/g-PEI was obtained, which is 30 times higher than that of the MCM-41 and more than twice that of the pure PEI. The experimental results showed that, although the dispersion of PEI on high surface area materials could increase the adsorption capacity, it was the synergetic effect between PEI and MCM-41 pore channels (CO_2 "molecular basket") that contributed to major increases in the CO_2 adsorption capacity. The uniform dispersion of the PEI into the pore channels of the MCM-41 support is critical for the preparation of this novel "molecular basket" adsorbent. Proper incorporation of Al into the MCM-41 framework in the synthesis step can significantly enhance the performance of the final MCM-41-PEI adsorbents. The relatively lower Si/Al ratio of the MCM-41 support and a relatively high methanol/MCM-41 weight ratio in adsorbent preparation can lead to higher CO_2 adsorption capacity for MCM-41-PEI. Adding polyethyleneglycol (PEG) into the MCM-41-PEI adsorbent can increase not only the CO_2 adsorption and desorption rates, but also the CO_2 adsorption capacity.

Carbon dioxide was successfully separated from a simulated flue gas mixture containing CO_2, O_2, N_2 and moisture by using the novel "molecular basket" adsorbent. The novel adsorbent showed a CO_2 adsorption capacity of 45.5 ml (STP)/g adsorbent and separation factors of above